THE PENNSYLVANIA STATE UNIVERSITY
SCHREYER HONORS COLLEGE

DEPARTMENT OF CHEMICAL ENGINEERING

An Exploration of the Role of Electrostatic Interactions on Monoclonal Antibody Behavior

THOMAS BUTTS
SPRING 2023

A thesis
submitted in partial fulfillment
of the requirements
for a baccalaureate degree
in Chemical Engineering
with honors in Chemical Engineering

Reviewed and approved* by the following:

Andrew Zydney
Bayard D. Kunkle Chair and Professor of Chemical Engineering
Thesis Supervisor

Ali Borhan
Professor of Chemical Engineering
Honors Adviser

* Electronic approvals are on file.

ABSTRACT

Monoclonal antibodies are an ever-growing sector within the pharmaceutical industry. These biologics offer novel, effective, and safe way of treating a variety of conditions and diseases. With the increasing demand for these treatments and the high concentration doses that are required for therapeutic use, it is imperative to make improvements in the manufacturing process used to make these proteins.

Virus removal filtration is currently one of the critical steps in protein purification insuring that the final therapeutic product is free of any contaminating viruses. However, many monoclonal antibodies cause significant filter fouling leading to decreased protein throughput. Investigating the behavior of monoclonal antibodies and their fouling phenomena are essential to optimizing the virus removal filtration processes. The objectives of this project are to evaluate the behavior of a model antibody and to develop an analytical lens by which to analyze other antibodies.

This project investigates the electrostatic interactions between monoclonal antibodies using added ionic compounds or charged excipients. The effects of adding Na_2SO_4, $CaCl_2$, NaCl, and L-Arginine to a model monoclonal antibody were studied experimentally. The data were analyzed based on the lyotropic properties of the salts, as described by the Hofmeister series, and the effective electrostatic shielding, as described by the Debye length.

The results of these experiments indicate that the Hofmeister series may provide a useful tool to predict aggregation behavior for proteins that have a pI greater than the solution pH. The Hofmeister series may provide a method for choosing which salts to add to monoclonal antibody solutions to improve stability and reduce aggregation. Further experimentation must be

conducted to determine the effect of the Debye length on the aggregation behavior and protein properties.

TABLE OF CONTENTS

LIST OF FIGURES

ACKNOWLEDGEMENTS

This thesis represents the culmination of months of hard work and would not have been possible without the invaluable support and guidance of the numerous individuals who have aided in my research. Firstly, I would like to thank Professor Andrew Zydney for providing me the opportunity to work on this exciting project and for serving as my thesis advisor. It is a privilege to be mentored by a world leading scientist in the field of membrane science. I will always be thankful for the knowledge and experience that I have gained under his tutelage.

I would like to express my sincere gratitude to my graduate mentor, (soon-to-be Dr.) Matthew Billups. Matt has played a critical role in my success as an undergraduate researcher and I am very thankful for the time and effort Matt has dedicated towards teaching me all about colloidal systems, mAbs, filtration membranes, and much more. I have met few people with the same passion and intellectual curiosity that Matt exhibits, both qualities that make him an exceptional and brilliant mentor. But more than anything else, I'm glad we made it through the day-long filtration experiments in one piece.

I would also like to express my heartfelt appreciation to my friends and family for their unending support during my education at Penn State, even when I bite off more than I can chew. Mom and dad, I will always be grateful for the support and guidance you have given me throughout my life—I would not be where I am today without your parenting. Brayden and Codey, I am extremely fortunate to be your older brother and I am very proud of all that you two have accomplished and continue to accomplish. To my friend Lexi, thank you for always being someone I can rely on when classes and other obligations begin to seem overwhelming. All of your support throughout my time at Penn State is more than I could ever ask for.

Finally, I would like to acknowledge Professor Janna Maranas. As the sole instructional aide for CHE 230 for the last few semesters, I had the pleasure to work closely with Janna. Fundamentally, Janna was endlessly kind-hearted. No matter what Janna was going through, she always made the effort to be there for others. Her compassion for others and teaching were self-evident and continue to be an inspiration to me today.

Chapter 1

Introduction of Monoclonal Antibodies

1.1 The Structure and Function of Antibodies

Antibodies are essential proteins used by the immune system to protect our bodies from various pathogens such as viruses and bacteria. These proteins are Y-shaped molecules with a molecular weight of approximately 150 kDa [1]. The structure of an antibody, seen in figure 1, is composed of two heavy chains (green) and two light chains (yellow). Each heavy chain is linked to a light chain and the two heavy chains are linked together via disulfide bonds (black) [2].

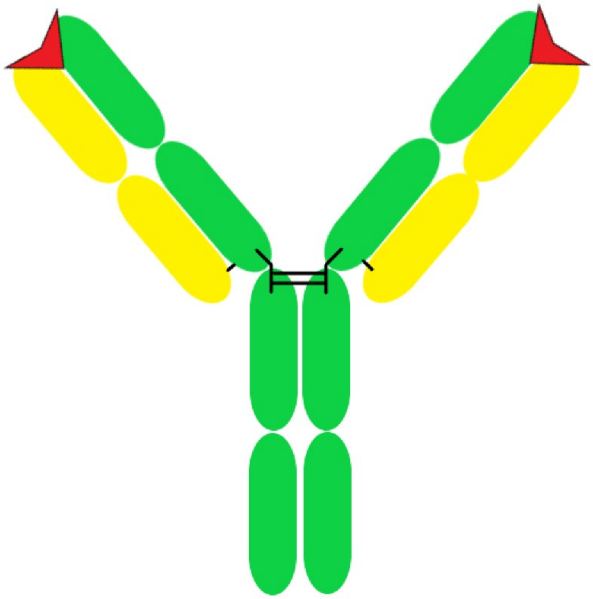

Figure 1. Antibody Structure.

Antibodies also contain a hypervariable region (red) that allows the antibodies to respond to different antigens (any foreign object in the body) encountered by the immune system [3]. These hypervariable regions allow antibodies to have a high degree of specificity (mono-

specificity) which enables the binding of each antibody to a specific epitope [4]. After attaching to the antigen, other immune cells can help destroy the pathogen via phagocytosis.

1.2 Applications of Antibodies

Ever since the generation of the first monoclonal antibody (mAb) in 1975, there has been an ever-growing interest in developing and commercializing mAbs for therapeutic purposes [5]. Over the last ~40 years, there has been a rapid development of therapeutic mAbs. The majority of mAbs fall into three therapeutic categories: oncological, immunological, or anti-infective [6]. In addition to their wide-ranging therapeutic capabilities, mAbs are particularly attractive biologics due to their safety and effectiveness.

As of 2022, there are over 80 therapeutic mAbs approved for use in the United States [4]. The global mAb market size was valued at 210.06 billion USD at the beginning of 2023 and is predicted to exhibit a compound annual growth rate of 11.04% from 2023 to 2030 [7]. Additionally, the COVID-19 pandemic has increased market expansion prospects by prompting the development of several mAbs used to treat the SARS-CoV-2 virus. Lastly, the scope of mAb applications is expected to continue its growth with the introduction of antibody fragments, antibody derivatives, and bispecific antibodies [7].

1.3 Viral Clearance for mAb Solutions

Due to the rapidly growing mAb industry and the increasing importance of mAb treatments for healthcare, it is imperative to optimize the various processes involved in the processing and purification of mAbs. One important step in the downstream processing of

products produced in mammalian cells is viral clearance. One particularly useful method of viral clearance is virus removal filtration. Virus removal filtration is a size-based approach to separating the therapeutic protein from viral contaminants and is commonly used in purification [8].

Virus filtration is a robust step for virus removal. Virus filtration membranes function by ensuring high viral clearance and acceptable protein throughput. Virus filtration is relatively insensitive to process conditions, but issues may arise when proteins form aggregates or there are other fouling species present in solution that cause the membrane to foul [9]. Significant protein fouling will result in decreased flux and reduced protein recovery.

One method of altering the extent of fouling is by changing the ionic strength of the solution. As seen in figure 2, an electrical double layer is formed around charged particles in aqueous solutions. The presence of the diffuse ion cloud surrounding the protein can cause the effective radius of the protein to be much larger than the hard sphere radius [10]. For example, the effective molecular weight of the protein can increase by a factor of more than 20 by changing the ionic strength of the solution from 150 to 5 mM [11]. The presence of an electrical double layer with a large radius can shield proteins from each other, resulting in reduced aggregation.

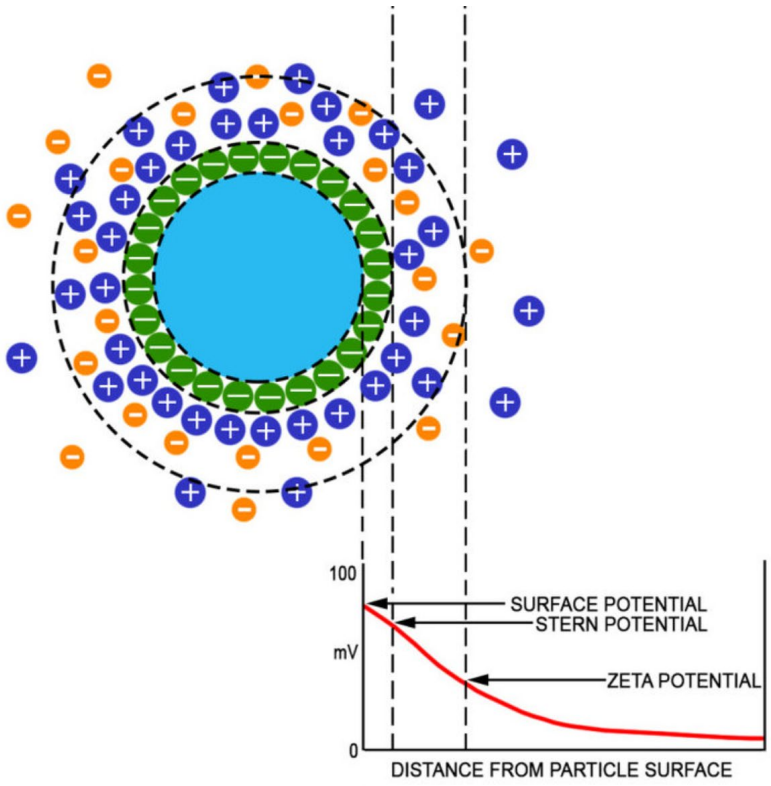

Figure 2. Model of the Electrical Double Layer Formed Around a Charged Particle [12].

1.4 Research Goals

The overarching goal of this project is to evaluate the impact of adding different salts or charged excipients to a mAb solution. Specifically, this project investigated:

- The impact of adding NaCl to mAb solution.
- The impact of adding Na_2SO_4 to mAb solution.
- The impact of adding $CaCl_2$ to Ab solution.
- The impact of adding L-Arginine to mAb solution.
- Estimate Debye length, κ^{-1}, for each salt solution.

- Evaluate usefulness of the Hofmeister series for understanding the effects of different salts on mAb aggregation and stability.

Chapter 2 will provide a broad overview of the methods and materials used to generate the experimental data. Chapter 3 will provide the results of the experiments performed. Chapter 4 will provide an analysis of the experimental data. Chapter 5 will explore the usefulness of the Hofmeister series for analyzing aggregation behavior. Chapter 6 will explore the usefulness of the Debye length for describing protein behavior in solution.

Chapter 2

Materials and Methods

2.1 Materials

Monoclonal Antibody:

All experiments were conducted using a mAb supplied by Bristol Myers Squibb. This mAb will hereon be referred to as “mAb-4”for consistency with other experimental studies. This mAb has a pI of 7.9 and is stored at a pH of 5.5. The concentration of the stock solution is approximately 23 g/L.

Buffer:

The buffer used throughout experimentation was a 40 mM citrate-phosphate buffer at a pH of 5.5 with a NaCl concentration of 100 mM. This buffer will be referred to as “mAb-4 buffer”.

Zetasizer Nano ZS:

The Zetasizer Nano ZS (Malvern Panalytical) is an instrument used to measure particle size of dispersed systems using the dynamic light scattering (DLS) technique [13]. Furthermore, this machine is capable of analyzing particle electrophoretic mobility and Zeta potential.

pH Meter:

The pH meter used to measure the pH of the L-Arginine stock solution was the PH800 Laboratory Benchtop pH Meter from APERA Instruments.

NaCl, Na_2SO_4, CaCl2, and L-Arginine:

The four additives used throughout experimentation were all sourced from Sigma-Aldrich. The additives came in crystalline form and had the following purities:

- NaCl: ACS reagent, ≥ 99%
- Na_2SO_4: ACS reagent, ≥ 99.0%
- $CaCl_2$: ≥ 97%
- L-Arginine: Reagent grade, ≥ 98%

2.2 DLS Measurements

There are a variety of measurements that can be taken by the Zetasizer Nano ZS. However, there are 3 main measurements that were used to analyze the mAb-4 properties.

Z-Average Diameter:

The Z-Average diameter is the intensity weighted mean hydrodynamic size of the ensemble collection of particles in a solution [14]. The Z-Average size is a preferred because it is less sensitive to noise. However, one downside to using the Z-Average diameter as an estimation of size is that large protein aggregates (even if there are only a few) can bias the Z-Average estimate. The size distribution by intensity graph must be checked to ensure that no significant aggregation is occurring.

Diffusion Coefficient:

The diffusion coefficient depends directly upon the size of the mAb. Since the size of the mAb directly correlates to the random Brownian motion of the protein, this value can give a good estimation of whether aggregation is occurring or not.

PDI:

The polydispersity index, or PDI, is a dimensionless value that indicates the breadth of the measured size distribution and in turn the reliability of the DLS-generated values. The DLS technique only provides reliable information for samples with relatively narrow size distributions, so the PDI provides a simple approach to indicate whether the data is reliable. If the Zetasizer reports a PDI of 0.7 or greater, then the sample has a broad size distribution and DLS technique is probably not suitable for that sample [15].

2.3 Methods

Procedure for NaCl Addition to mAb-4:

Create a 200 mM NaCl + mAb-4 buffer solution by weighing and adding appropriate mass of NaCl to mAb-4 buffer. Then, perform a set of serial dilutions to create three more buffer solutions:

i. 150 mM NaCl + mAb-4 buffer

ii. 100 mM NaCl + mAb-4 buffer

iii. 50 mM NaCl + mAb-4 buffer

Then, combine each of the buffer solutions separately with sterile filtered mAb-4 stock to obtain solutions with mAb-4 concentrations of ~15 g/L. Then perform 3 sets of serial dilutions to obtain

solutions with mAb-4 concentrations of 10 g/L, 6 g/L, and 4 g/L. In total, 16 solutions will be created. Finally, ~65 μL of each solution will be pipetted into the Zetasizer. The Z-Average size, Diffusion Coefficient, and PDI will be measured for each sample.

Procedure for Na_2SO_4 Addition to mAb-4:

Create a 200 mM Na_2SO_4 + mAb-4 buffer solution by weighing and adding appropriate mass of Na_2SO_4 to mAb-4 buffer. Then, perform a set of serial dilutions to create three more buffer solutions:

i. 150 mM Na_2SO_4 + mAb-4 buffer

ii. 100 mM Na_2SO_4 + mAb-4 buffer

iii. 50 mM Na_2SO_4 + mAb-4 buffer

Then, combine each of the buffer solutions separately with sterile filtered mAb-4 stock to obtain solutions with a mAb-4 concentrations of ~15 g/L. Then perform 3 sets of serial dilutions to obtain solutions with mAb-4 concentrations of 10 g/L, 6 g/L, and 4 g/L. In total, 16 solutions will be created. Finally, ~65 μL of each solution will be pipetted into the Zetasizer. The Z-Average size, Diffusion Coefficient, and PDI will be measured for each sample.

Procedure for $CaCl_2$ Addition to mAb-4:

Create a 200 mM $CaCl_2$ + mAb-4 buffer solution by weighing and adding appropriate mass of $CaCl_2$ to mAb-4 buffer. Then, perform a set of serial dilutions to create three more buffer solutions:

i. 150 mM $CaCl_2$ + mAb-4 buffer

ii. 100 mM $CaCl_2$ + mAb-4 buffer

iii. 50 mM $CaCl_2$ + mAb-4 buffer

Then, combine each of the buffer solutions separately with sterile filtered mAb-4 stock to obtain solutions with mAb-4 concentrations of ~15 g/L. Then perform 3 sets of serial dilutions to obtain solutions with mAb-4 concentrations of 10 g/L, 6 g/L, and 4 g/L. In total, 16 solutions will be created. Finally, ~65 μL of each solution will be pipetted into the Zetasizer. The Z-Average size, Diffusion Coefficient, and PDI will be measured for each sample.

Preparation of L-Arginine Solution and pH Adjustment:

Weigh out appropriate mass of L-Arginine to form a 1 M L-Arginine + mAb-4 buffer solution. Then, use a sonication bath to ensure complete dissolution of L-Arginine. Finally, use a pH meter and 5 M HCl to adjust the pH to ~5.5.

Procedure for Addition of L-Arginine to mAb-4:

Create a 0.84 M L-Arginine + mAb-4 buffer solution by weighing and adding appropriate mass of L-Arginine to mAb-4 buffer. Then, perform a set of serial dilutions to create three more buffer solutions.

i. 0.25 M L-Arginine + mAb-4 buffer

ii. 0.10 M L-Arginine + mAb-4 buffer

iii. 0.025 M L-Arginine + mAb-4 buffer

Then, combine each of the buffer solutions with sterile filtered mAb-4 stock to obtain solutions with mAb-4 concentrations of ~15 g/L. Then perform 3 sets of serial dilutions to obtain solutions

with mAb-4 concentrations of 10, 6 , and 4 g/L. In total, 16 solutions will be created. Finally, ~65 μL of each solution will be pipetted into the Zetasizer. The Z-Average size, Diffusion Coefficient, and PDI will be measured for each sample.

Chapter 3

Experimental Results

NaCl Addition to mAb-4:

DLS measurements were performed on each mAb + NaCl solution to generate values for the Z-Average size and diffusion coefficients. Figure 3 shows the Z-Average diameter as a function of the concentration of mAb-4 for the different NaCl concentrations and figure 4 shows the corresponding data for the diffusion coefficients.

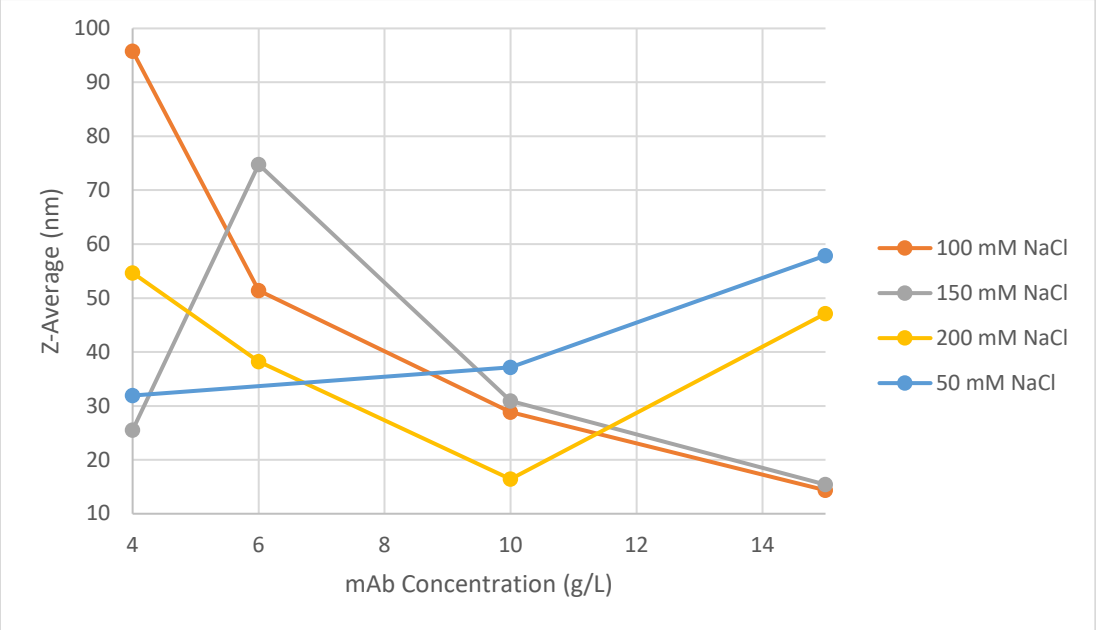

Figure 3. Z-Average diameter for mAb-4 in the presence of different NaCl concentrations.

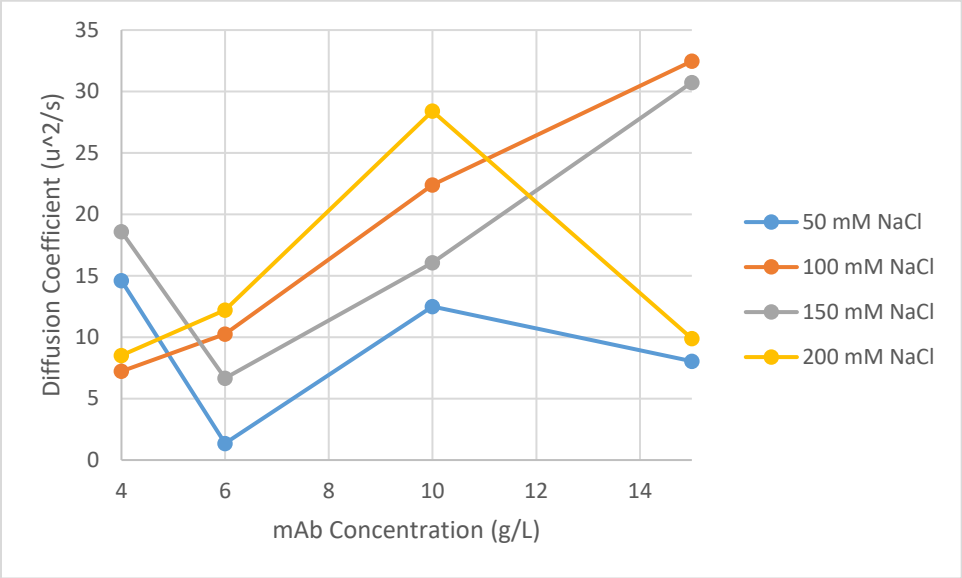

Figure 4. Diffusion Coefficients for mAb-4 + NaCl.

The data obtained for the Z-Average diameter and diffusion coefficient values for mAb-4 in the presence of different NaCl concentrations do not show any consistent trends. The largest diameter was obtained in the 100 mM NaCl for the 4 g/L mAb concentration, while the smallest diameter was obtained in the 200 mM NaCl for the 10 g/L mAb concentration. Furthermore, all the data exhibited significant aggregation of mAb-4; the expected diameter of the monoclonal antibody should be around 10 nm. Appendix A provides examples of the intensity size distribution with the graphs containing multiple peaks.

Na_2SO_4 Addition to mAb-4:

DLS measurements were also performed on each mAb + Na_2SO_4 solution with results shown in Figure 5 for the Z-Average diameter and Figure 6 for the diffusion coefficient.

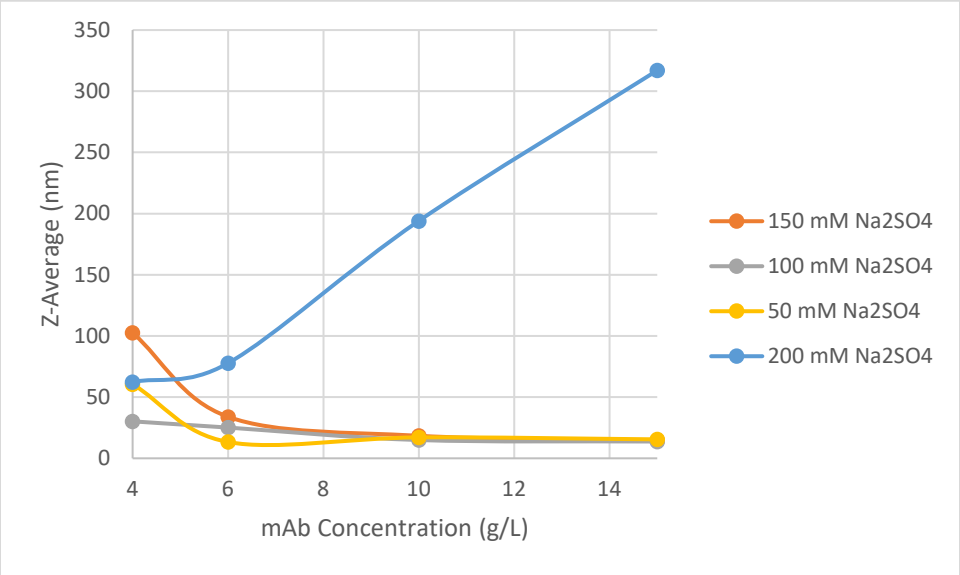

Figure 5. Z-Average diameter for mAb-4 in different Na_2SO_4 solutions.

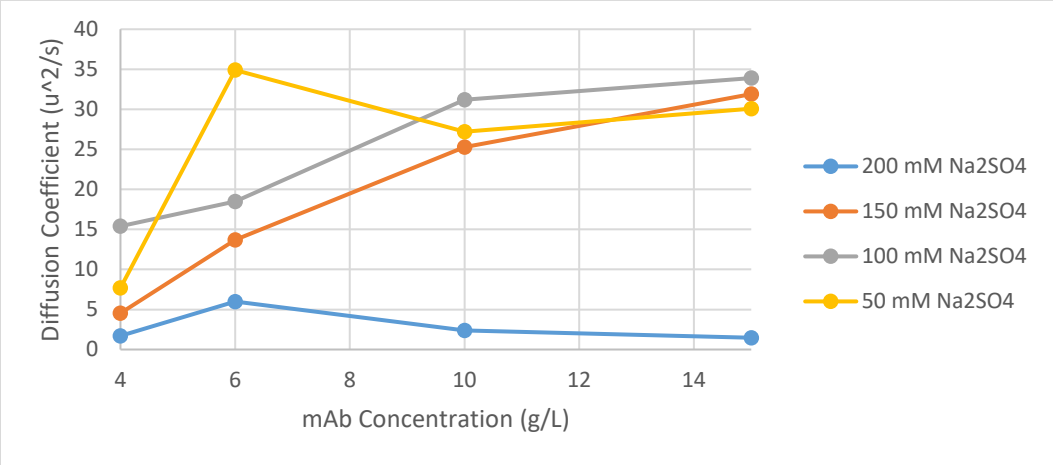

Figure 6. Diffusion Coefficients for mAb-4 in different Na_2SO_4 solutions.

The high Z-Average diameters in thef 200 mM Na_2SO_4 suggests that this set of buffer conditions induces significant aggregation. This is in sharp contrast to the data for the other concentrations of Na_2SO_4. Similar behavior is seen in Figure 6 for the diffusion coefficients. Appendix A provides examples of the intensity size distribution.

$CaCl_2$ Addition to mAb-4:

DLS measurements were then performed on the mAb in $CaCl_2$ solutions. Figure 7 shows the Z-Average diameter as a function of the mAb-4 concentration of mAb-4 in different $CaCl_2$ solutions and figure 8 shows the corresponding diffusion coefficients.

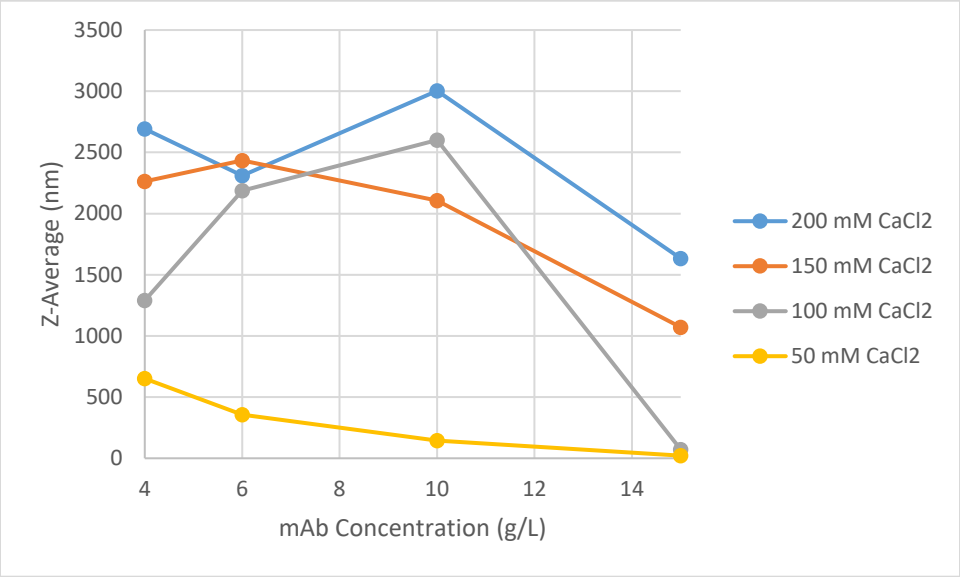

Figure 7. Z-Average for mAb-4 + $CaCl_2$.

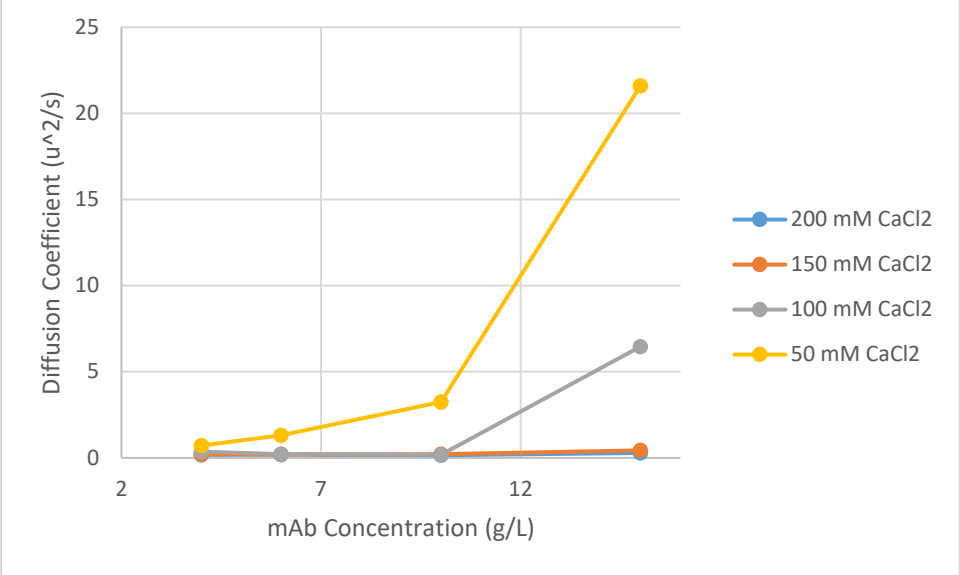

Figure 8. Diffusion Coefficients for mAb-4 + $CaCl_2$.

The data obtained for the Z-Average diameter and diffusion coefficients show no clear pattern. The data suggest significant aggregation at all concentrations of $CaCl_2$. Refer to appendix A for examples of the intensity size distribution. All intensity graphs showed multiple peaks, which makes it difficult to interpret the DLS results. Furthermore, small white precipitates were observed to form upon adding $CaCl_2$ to the mAb-4 solution. It is possible that these precipitates are associated with salting out of the proteins from the $CaCl_2$ solution.

L-Arginine Addition to mAb-4:

Unlike NaCl, Na_2SO_4, and $CaCl_2$ (which are all inorganic ionic compounds), L-Arginine is an organic charged excipient. L-Arginine, as seen in figure 9, is a naturally occurring amino acid that has been used as a stabilizing additive for biologics [16].

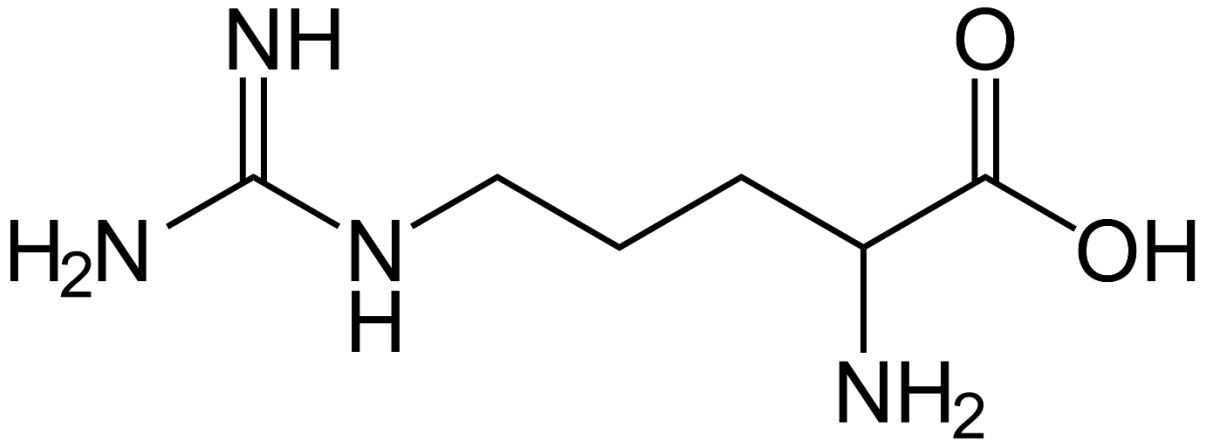

Figure 9. Structure of L-Arginine.

DLS measurements were performed on the mAb in L-Arginine solutions to evaluate the Z-Average size and diffusion coefficients in Figure 10 and figure 11, respectively..

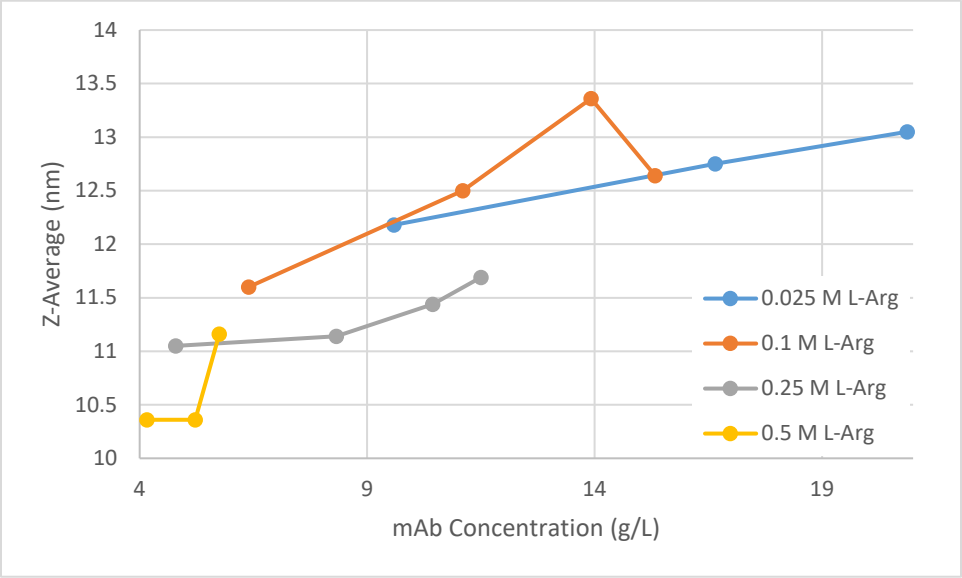

Figure 10. Z-Averages for mAb-4 + L-Arginine.

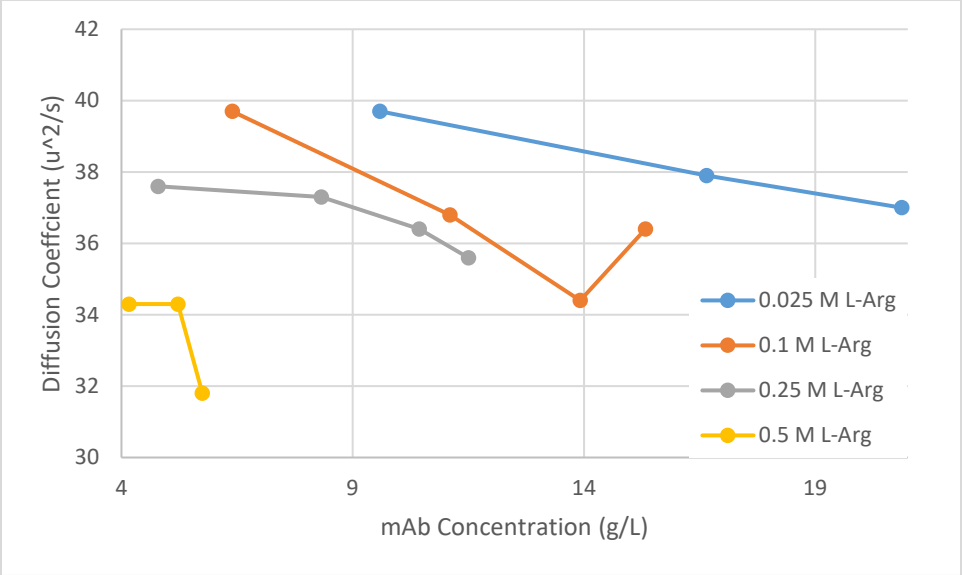

Figure 11. Diffusion Coefficients for mAb-4 + L-Arginine.

In contrast to the data in the inorganic salt solutions, the Z-average size for mAb-4 in L-arginine was between 10 and 13.5 nm, values that are consistent with the expected size of an antibody molecule. Figures 10 and 11 indicate that there is a correlation between the L-Arginine concentration and the Z-Average size. Generally, the higher the concentration of L-Arginine, the

smaller the Z-Average size is for that sample. Furthermore, no significant aggregation was observed at any concentration of mAb-4 or L-Arginine.

Chapter 4

Experimental Data Analysis

Salt Additions to mAb-4:

Generally, the addition of salt to mAb-4 was unsuccessful in decreasing the Z-Average size of the antibodies in solution. Instead, the addition of $CaCl_2$ and NaCl (at the tested concentrations) appeared to cause significant aggregation in the protein solutions. Furthermore, Na_2SO_4 at a concentration of 200 mM or more also caused significant aggregation. It may be the case that this mAb is particularly sensitive to the addition of ionic compounds since the buffer already has 100 mM NaCl. The addition of more ions into solution may be shielding the repulsive interactions between the proteins causing the mAb to readily aggregate.

L-Arginine Addition to mAb-4:

The addition of L-Arginine was far more successful in producing promising results than the addition of salts. The addition of L-Arginine did not cause aggregation at any concentration. Furthermore, the Z-average size appeared to decreasing with increasing concentration of L-Arginine, suggesting that the L-arginine may be stabilizing the individual antibody molecules thereby reducing self-association between the mAb..

Recommendations for Future Experimentation with mAb-4:

There are two major experiments that should be tested in the future to further evaluate the potential for L-Arginine and Na_2SO_4 to reduce membrane fouling during virus removal filtration:

1. Filtration of mAb-4 + ≤150 mM Na_2SO_4: The flux behavior of mAb-4 through a virus removal filter (e.g., the Pegasus SV4 virus removal filter) should be analyzed at various concentrations of Na_2SO_4. The concentration of Na_2SO_4 should be no more than 150 mM.
2. Filtration of mAb-4 + L-Arginine: The flux behavior of mAb-4 through a virus removal filter (e.g., the Pegasus SV4 virus removal filter) should be analyzed for L-Arginine concentrations of 0.025, 0.1, 0.25, and 0.5 M. If initial experiments indicate that the addition of L-Arginine improves the filtration flux, it may be worth increasing the concentration of L-Arginine beyond 0.5 M.

Chapter 5

Hofmeister Series Analysis

The Hofmeister series (also known as the lyotropic series) is a classification of ions in order of their ability to salt in or salt out proteins [17]. This series may be viewed in figure 12 below.

ANIONS:

$$F^- \approx SO_4^{2-} > HPO_4^{2-} > C_2H_3O_2^- > Cl^- > Br^- > NO_3^- > ClO_3^- > I^- > ClO_4^- > SCN^-$$

CATIONS:

$$NH_4^+ > K^+ > Na^+ > Li^+ > Mg^{2+} > Ca^{2+}$$

Figure 12. Hofmeister Series [18].

The ions on the left side of figure 12 have a greater ability to salt out or precipitate proteins out of solution. This ordering would seem to suggest that salts such as Na_2SO_4 have the greatest ability to salt out proteins since NH_4^- and Na^+ are both on the left side of the Hofmeister series. Similarly, this ordering would seem to suggest that $CaCl_2$ has little ability to salt out a protein since Ca^{2+} and Cl^- are further to the right of the series. However, this series is most commonly observed when the protein bears a net negative charge.

For the case of mAb-4, the pI is 7.9 and the pH of the solutions examined in this work is 5.5. Since the pH is less than the pI, the protein will bear a net positive charge, which is typical of most commercial mAbs. When the protein bears a net positive charge, a reverse Hofmeister series will be observed [18]. This aligns directly with the experimental evidence gathered during the experiments conducted in this thesis. $CaCl_2$ and NaCl both induced significant aggregation

and $CaCl_2$ even led to the development of small white precipitates. Furthermore, addition of Na_2SO_4 caused lower levels of aggregation; Na_2SO_4 did not induce significant aggregation until concentrations of 200 mM were added.

The salt addition experiments suggest that the Hofmeister series may be a good tool for researchers to use in the future to analyze monoclonal antibodies and to select salts that may be effective in reducing aggregation in protein solutions. Instead of randomly evaluating the effects of adding different salts, the Hofmeister series offers an analytical framework that can tell researchers which salts may be worth investigating for reducing fouling behaviors.

Further experiments must be conducted to ensure that the increase in Z-Average size observed in each salt addition corresponds to a decrease in filtration flux during virus removal filtration. Further salt-addition experiments must also be conducted for other mAbs to ensure that this phenomenon is a universal property observed with proteins and that this is not unique to mAb-4.

When considering the impact of adding L-Arginine to the mAb-4 solution, it is important to remember that L-Arginine will exist as a net-positive molecule (since pH < pI). It is also important to remember that the mAb-4 stock solution contains 100 mM NaCl already. This means that the positively-charged L-Arginine will likely be associated with the negatively-charged Cl^- ions in solution. It is thus possible that L-Arginine lowers the Z-Average size and the extent of protein aggregation by reducing the impact of the "harmful" Cl^- ions in solution.

Chapter 6

Debye Length Analysis

Electrical Double Layer (EDL):

The electrical double layer is a key concept in colloid science and the study of colloidal forces. The EDL refers to the two charged layers that surround a particle. The first charged layer is the fixed layer of charges that are effectively attached to the particle surface. The second charged layer is the fluid layer adjacent to the particle surface and is composed of "counter-ions" that have an opposite charge of the first layer [19]. A visualization of the EDL can be viewed in figure 13 below.

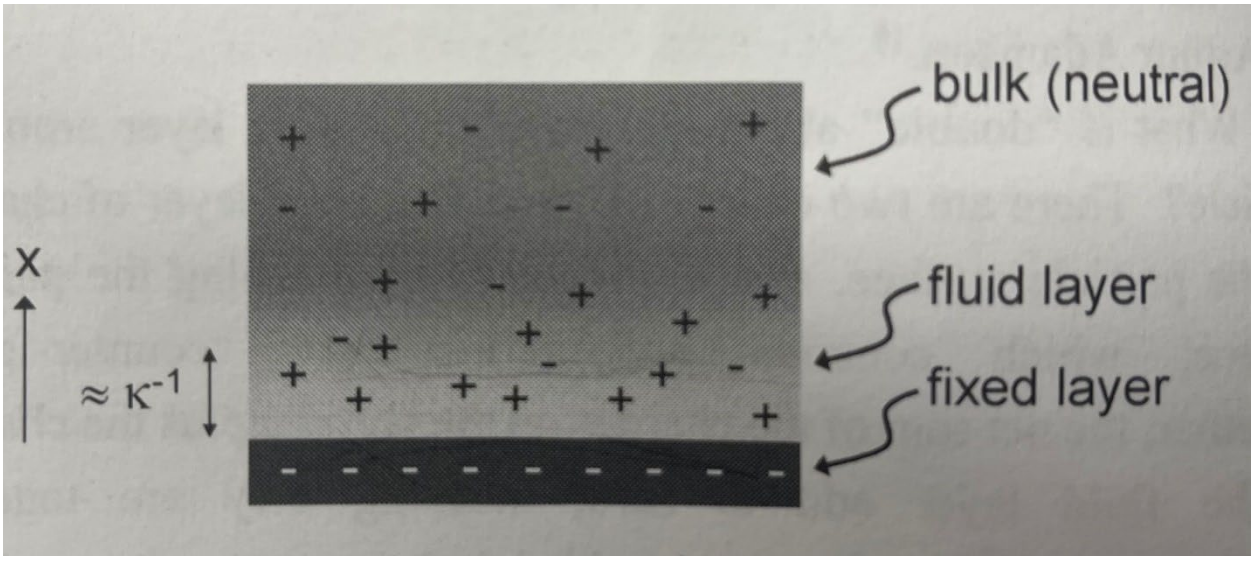

Figure 13. Electrical Double Layer (EDL). Stern Layer is Excluded from Graphic [19].

Another important parameter in colloidal science is the Debye length, κ^{-1}. This length plays an important role in determining the magnitude of the electrostatic potential neat the surface of the charged particle. The Debye length may be evaluated from equation 1:

$$\kappa^2 = \sum_{i=1}^{N} \frac{Z_i^2 e^2 c_{\infty,i}}{\varepsilon k T} \tag{1}$$

where Z_i is the charge of the ion. For example, Z_{Cl} for $CaCl_2$ would be equal to 1 and Z_{Ca} would be equal to 2. Solving for the Debye length of the $CaCl_2$ solution results in the following:

$$\kappa^2 = \frac{Z_{Ca}^2 e^2 C_{\infty,Ca}}{\varepsilon k T} + \frac{Z_{Cl}^2 e^2 C_{\infty,Cl}}{\varepsilon k T} \tag{2}$$

Assuming $C_{\infty,Ca} = C_{\infty}$ and $C_{\infty,Cl} = 2 * C_{\infty}$, the expression simplifies to

$$\kappa^2 = \frac{2^2 * e^2 C_{\infty}}{\varepsilon k T} + \frac{1^2 * e^2 C_{\infty}}{\varepsilon k T} \tag{3}$$

or

$$\kappa^2 = \frac{4 * e^2 C_{\infty}}{\varepsilon k T} + \frac{e^2 C_{\infty}}{\varepsilon k T} = \frac{5 * e^2 C_{\infty}}{\varepsilon k T} \tag{4}$$

Solving for the Debye length gives

$$\kappa_{CaCl_2}^{-1} = \frac{1}{\sqrt{\frac{5 e^2 C_{\infty}}{\varepsilon k T}}} \tag{5}$$

The corresponding equations for the Debye length of NaCl and Na_2SO_4 solutions are:

$$\kappa_{NaCl}^{-1} = \frac{1}{\sqrt{\frac{2 e^2 C_{\infty}}{\varepsilon k T}}} \tag{6}$$

$$\kappa_{Na_2SO_4}^{-1} = \frac{1}{\sqrt{\frac{5 * e^2 C_{\infty}}{\varepsilon k T}}} \tag{7}$$

Note that the ratio of the Debye length in a Na_2SO_4 solution to that in a $CaCl_2$ solution of the same molarity is a constant:

$$\frac{\kappa^{-1}_{Na_2SO_4}}{\kappa^{-1}_{CaCl_2}} = \frac{\frac{1}{\sqrt{\frac{5 * e^2 C_\infty}{\varepsilon k T}}}}{\frac{1}{\sqrt{\frac{5 e^2 C_\infty}{\varepsilon k T}}}} = 1 \qquad (8)$$

Thus, the largest Debye length is obtained in a NaCl solution, followed by $CaCl_2$ and Na_2SO_4. A visual representation of the relative Debye lengths in the different salt solutions can be viewed in figure 13.

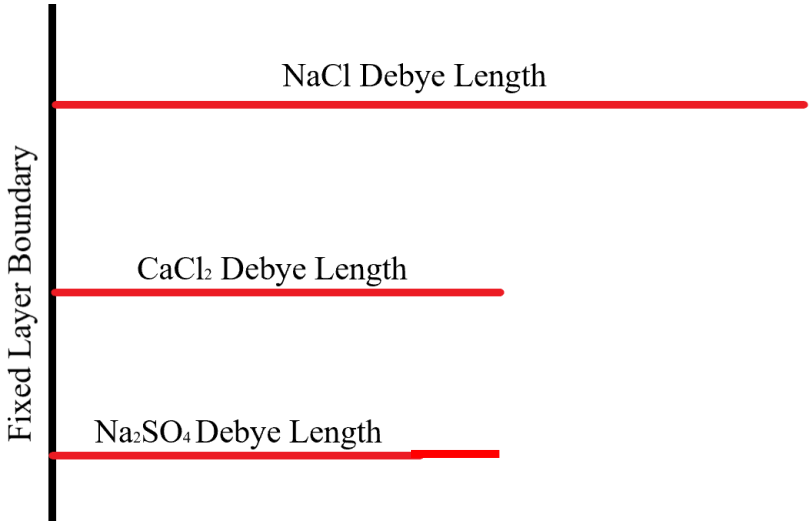

Figure 14. Relative Debye Lengths in Solutions of NaCl, $CaCl_2$, and Na_2SO_4.

If an increase in the Debye length leads to protein aggregation, then Figure 14 suggests that proteins in solutions of NaCl, which has a longer Debye lengths and thus greater electrostatic repulsion between mAbs, should show less aggregation. However, further experimentation is required to determine if this type of relationship between aggregation and Debye length exists for mAb-4. Furthermore, filtration experiments will need to be conducted to

determine if increasing the salt concentration has a positive or negative impact on the filtration flux during virus removal filtration.

Chapter 7

Conclusions

With the continuous development and popularization of monoclonal antibody treatments, the biotechnology industry has been pushing for technological improvements to the purification and membrane processes used to produce these life-saving therapeutics. Virus removal membranes can struggle to properly purify therapeutic proteins from viruses due to some proteins' tendency to aggregate. One such protein, mAb-4, was evaluated during this thesis to better understand the role of electrostatic interactions on the aggregation behavior. This thesis presented data relating to the Z-Average size and diffusion coefficients upon addition of various charged excipients with the goal of establishing an analytical lens by which other monoclonal antibodies can be studied.

Dynamic light scattering experiments were conducted with mAb-4 in the presence of 3 different salts: NaCl, Na_2SO_4, and $CaCl_2$. Various samples were tested, each with a different concentration of mAb-4 and salt. Z-Average sizes were measured using the Zetasizer Nano ZS from Malvern Panalytical. Dynamic light scattering experiments were also conducted with mAb-4 in the presence of L-Arginine.

Results from these experiments established that $CaCl_2$ and NaCl additions promoted protein aggregation at all tested concentrations. In contrast, Na_2SO_4 only caused protein aggregation at high concentrations. The addition of L-Arginine to the solution had a positive

impact on the Z-Average size, with high concentrations of L-Arginine causing lower Z-Average diameters.

Thereafter, two approaches were used to analyze the effects of different salts on the aggregation behavior of monoclonal antibodies. Firstly, the Hofmeister series was used to compare the effect of the salt additions. Since the pH of the solutions examined in this these were less than the isoelectric point of the mAb, a reverse Hofmeister series appeared to effectively describe the relative aggregation behavior in the different salt solutions. Furthermore, L-Arginine appears to be a very effective excipient because it will associate with ions that are likely to induce aggregation.

Secondly, the Debye length was evaluated for the different salt solutions in an attempt to understand the different aggregation behavior. However, the Debye length does not appear to be a particularly effective analytical lens for examining the effects of the different salts, although it might prove to be useful if more salts were studied over a broader range of conditions. The $CaCl_2$ and Na_2SO_4 calculations had the same Debye lengths, but the observed aggregation behavior was quite different, indicating that the Debye length alone does not strongly correlate with the protein's aggregation behavior. Further experiments would need to be conducted to determine the usefulness of the Debye length as an indicator of the aggregation behavior of mAb-4.

Appendix A

Size Distribution by Intensity for mAb-4 in Various Salt Solutions

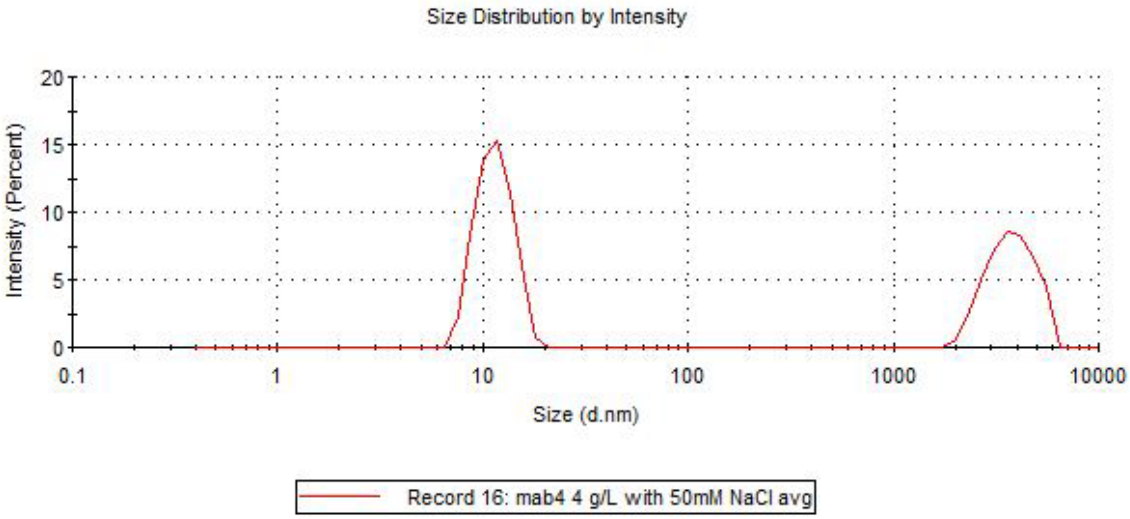

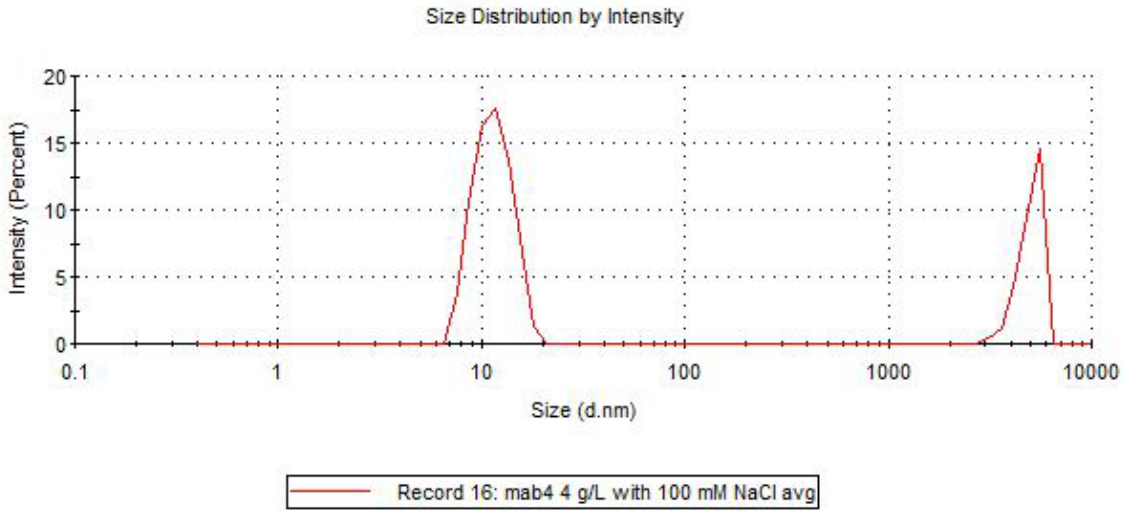

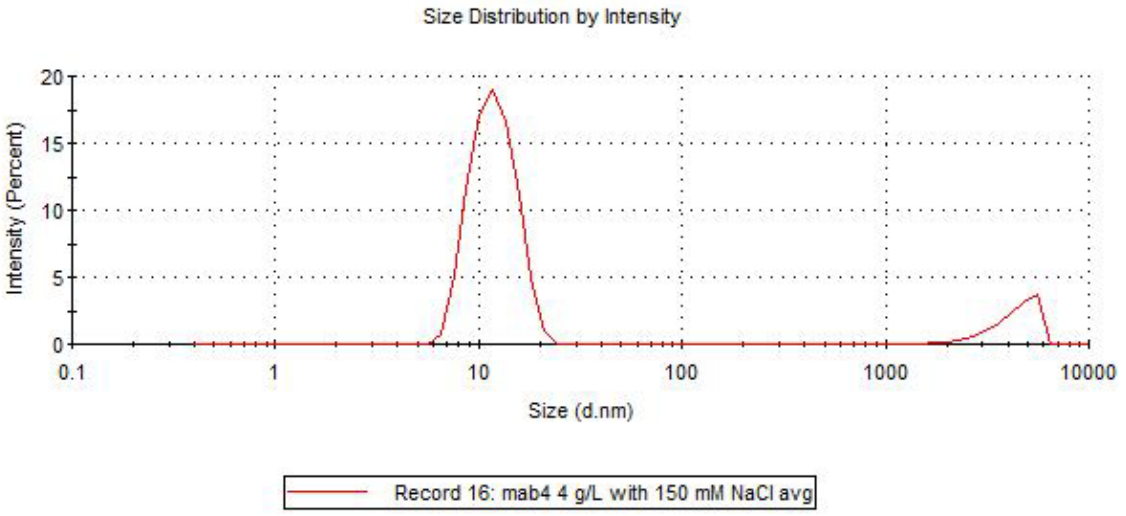
Size Distribution by Intensity
Intensity (Percent)
20
15
10
5
0
0.1
1
10
100
1000
10000
Size (d.nm)
Record 16: mab4 4 g/L with 150 mM NaCl avg

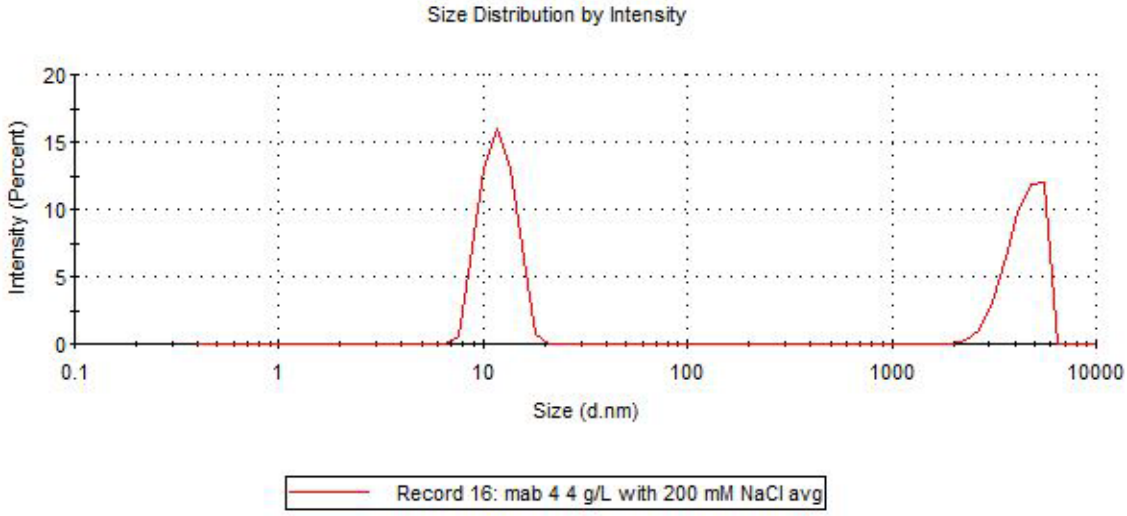
Size Distribution by Intensity
Intensity (Percent)
20
15
10
5
0
0.1
1
10
100
1000
10000
Size (d.nm)
Record 16: mab 4 4 g/L with 200 mM NaCl avg

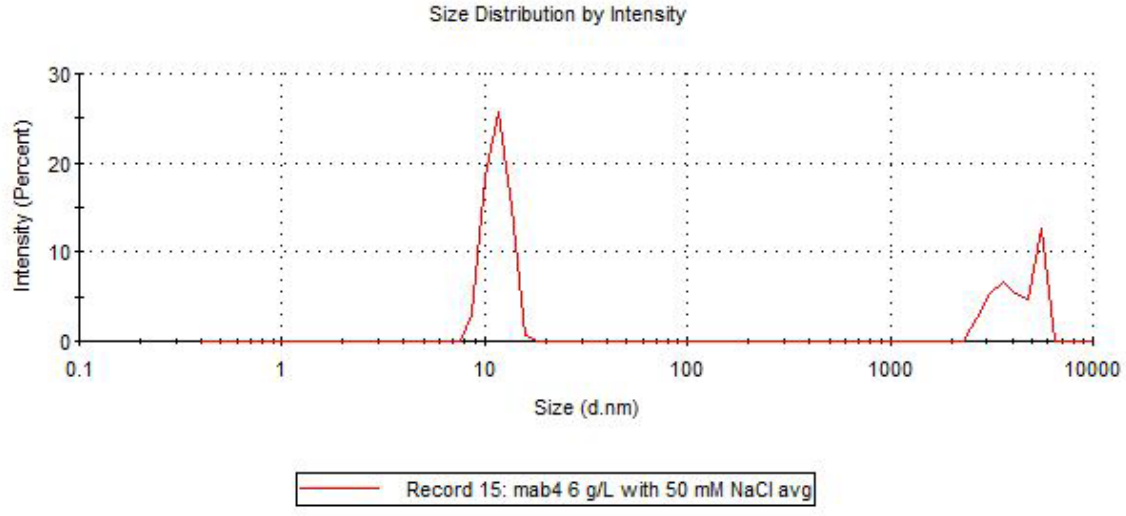
Size Distribution by Intensity
Intensity (Percent)
30
20
10
0
0.1
1
10
100
1000
10000
Size (d.nm)
Record 15: mab4 6 g/L with 50 mM NaCl avg

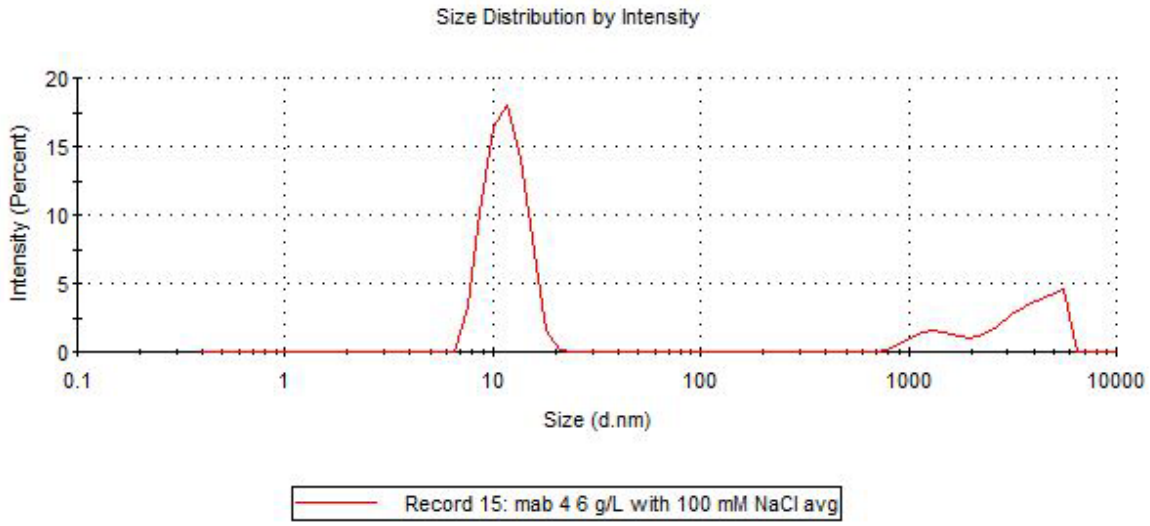
Size Distribution by Intensity
Intensity (Percent)
20
15
10
5
0
0.1
1
10
100
1000
10000
Size (d.nm)
Record 15: mab 4 6 g/L with 100 mM NaCl avg

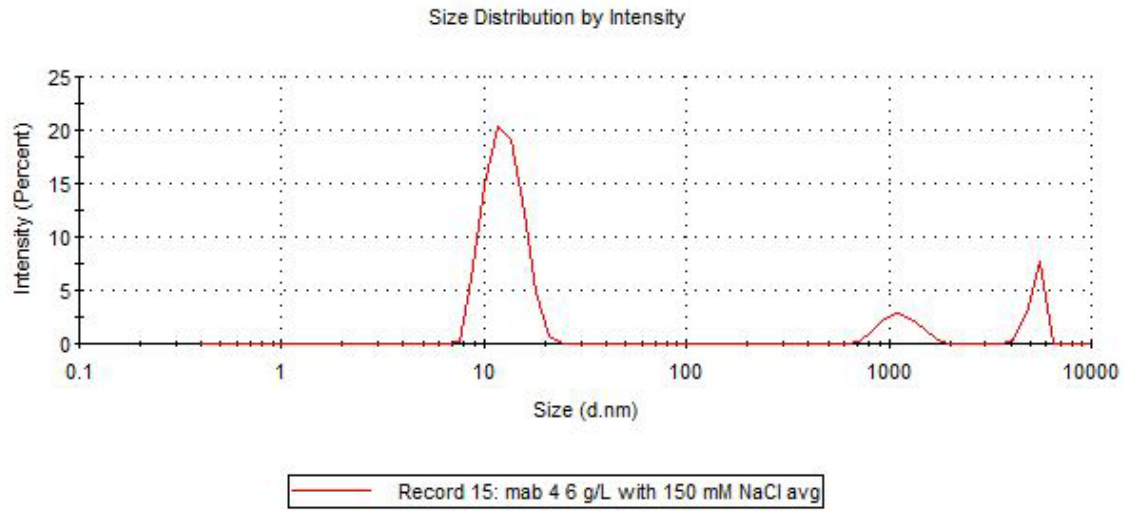
Size Distribution by Intensity
Intensity (Percent)
25
20
15
10
5
0
0.1
1
10
100
1000
10000
Size (d.nm)
Record 15: mab 4 6 g/L with 150 mM NaCl avg

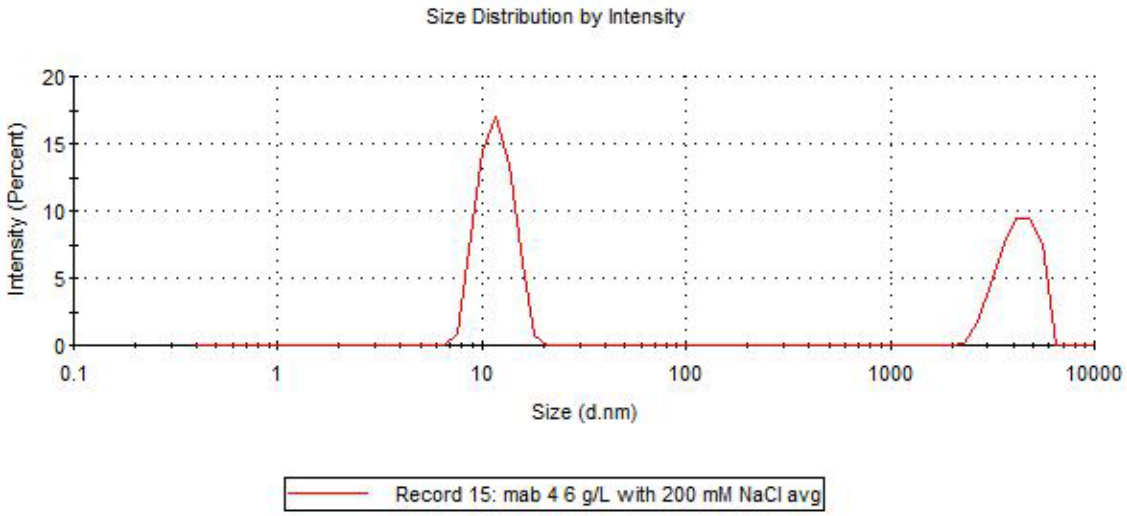
Size Distribution by Intensity
Intensity (Percent)
20
15
10
5
0
0.1
1
10
100
1000
10000
Size (d.nm)
Record 15: mab 4 6 g/L with 200 mM NaCl avg

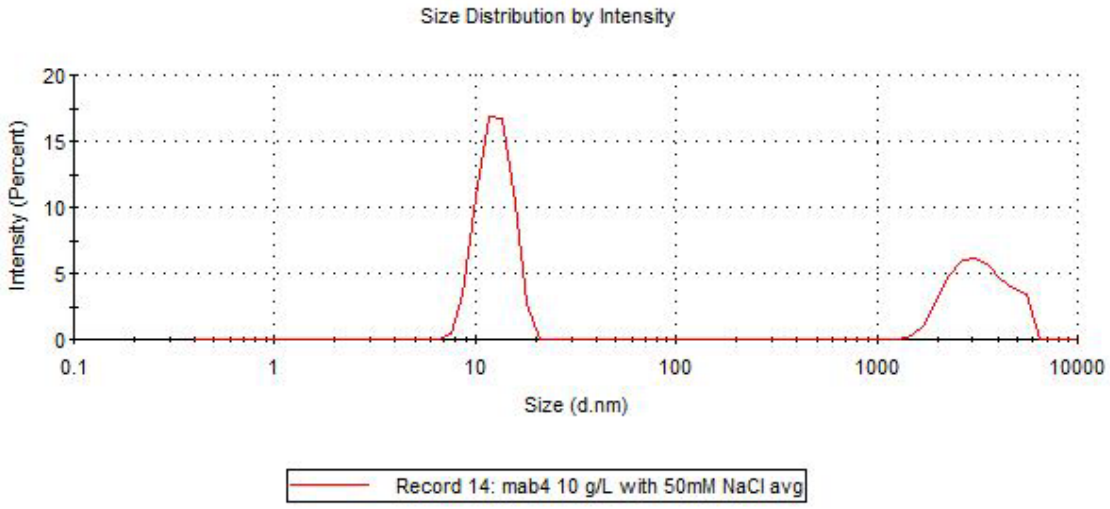
Size Distribution by Intensity
Intensity (Percent)
20
15
10
5
0
0.1
1
10
100
1000
10000
Size (d.nm)
Record 14: mab4 10 g/L with 50mM NaCl avg

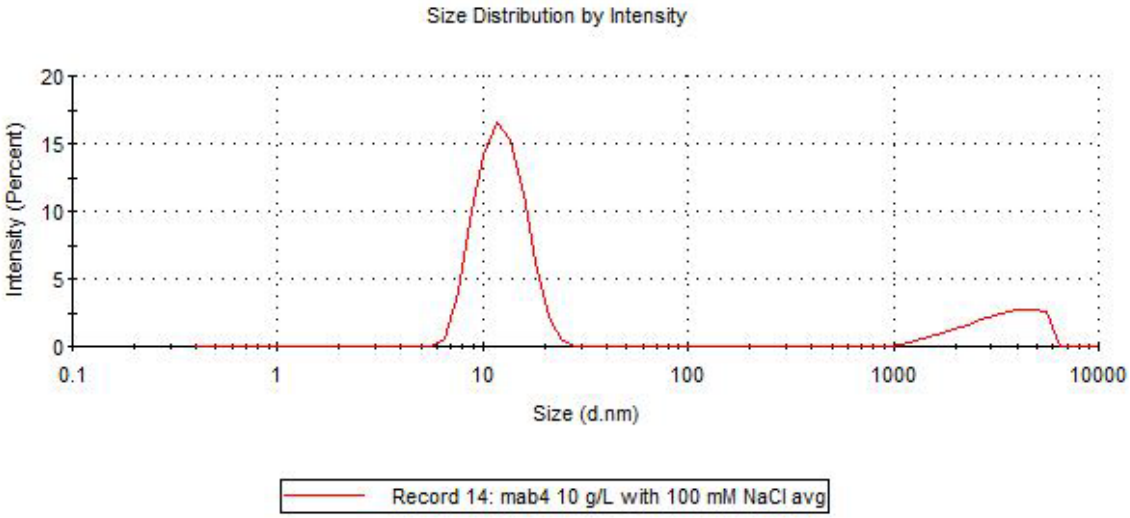
Size Distribution by Intensity
Intensity (Percent)
20
15
10
5
0
0.1
1
10
100
1000
10000
Size (d.nm)
Record 14: mab4 10 g/L with 100 mM NaCl avg

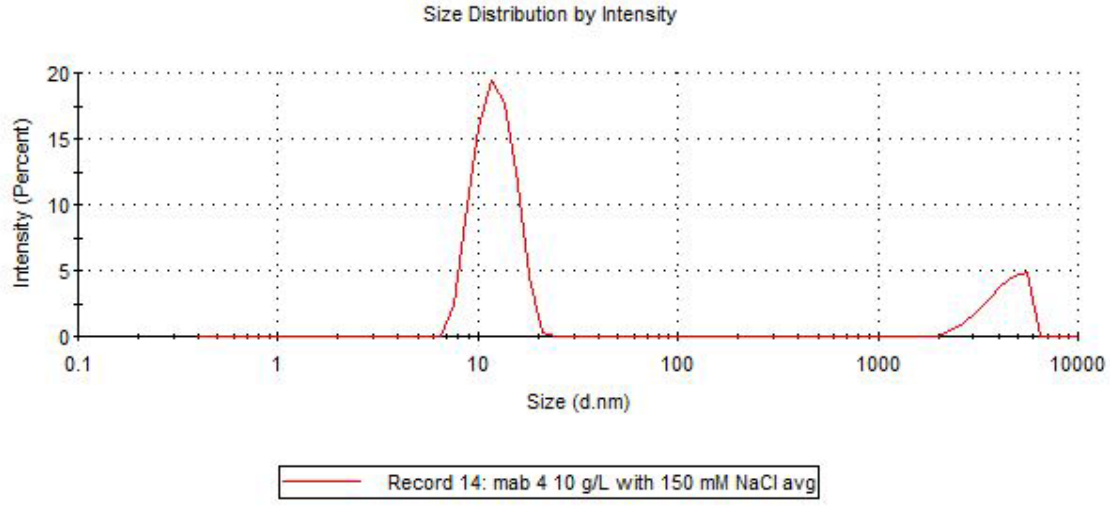
Size Distribution by Intensity
Intensity (Percent)
20
15
10
5
0
0.1
1
10
100
1000
10000
Size (d.nm)
Record 14: mab 4 10 g/L with 150 mM NaCl avg

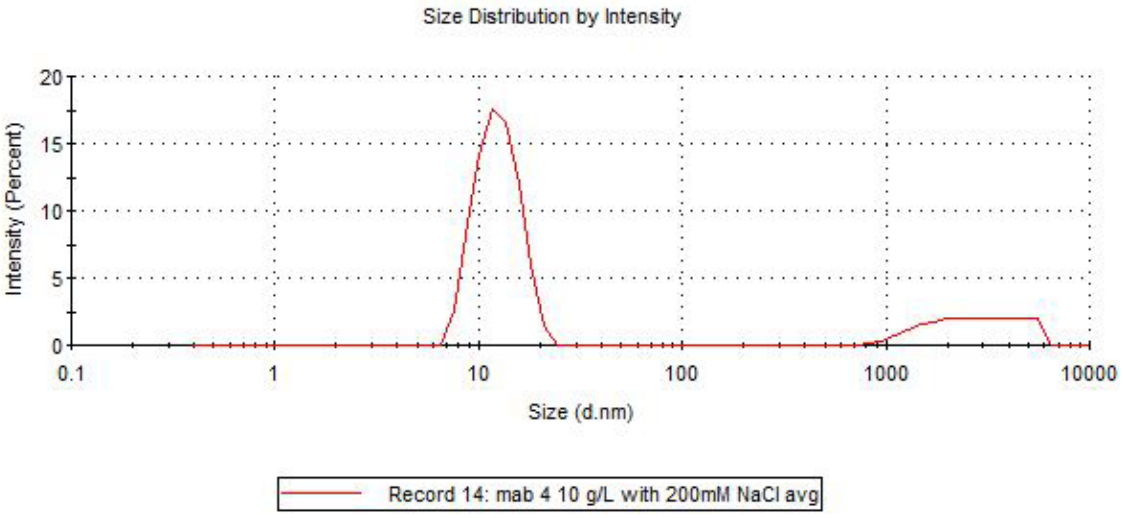
Size Distribution by Intensity
Intensity (Percent)
20
15
10
5
0
0.1
1
10
100
1000
10000
Size (d.nm)
Record 14: mab 4 10 g/L with 200mM NaCl avg

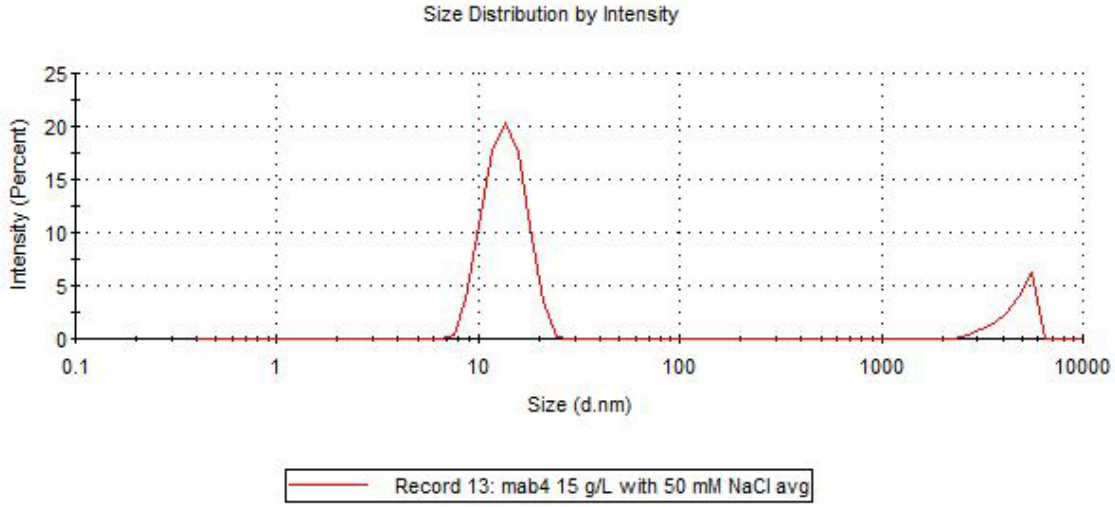
Size Distribution by Intensity
Intensity (Percent)
25
20
15
10
5
0
0.1
1
10
100
1000
10000
Size (d.nm)
Record 13: mab4 15 g/L with 50 mM NaCl avg

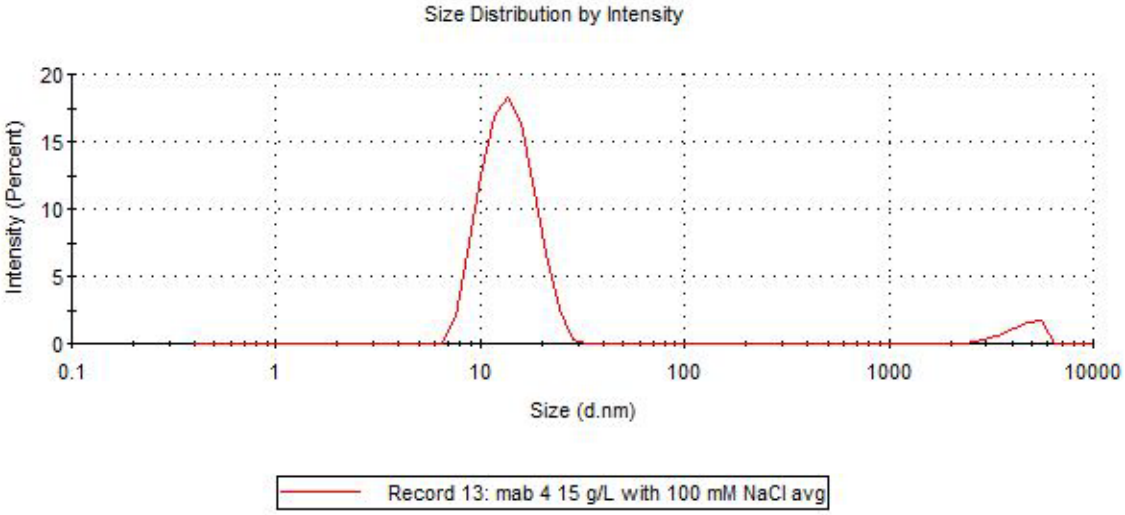
Size Distribution by Intensity
Intensity (Percent)
20
15
10
5
0
0.1
1
10
100
1000
10000
Size (d.nm)
Record 13: mab 4 15 g/L with 100 mM NaCl avg

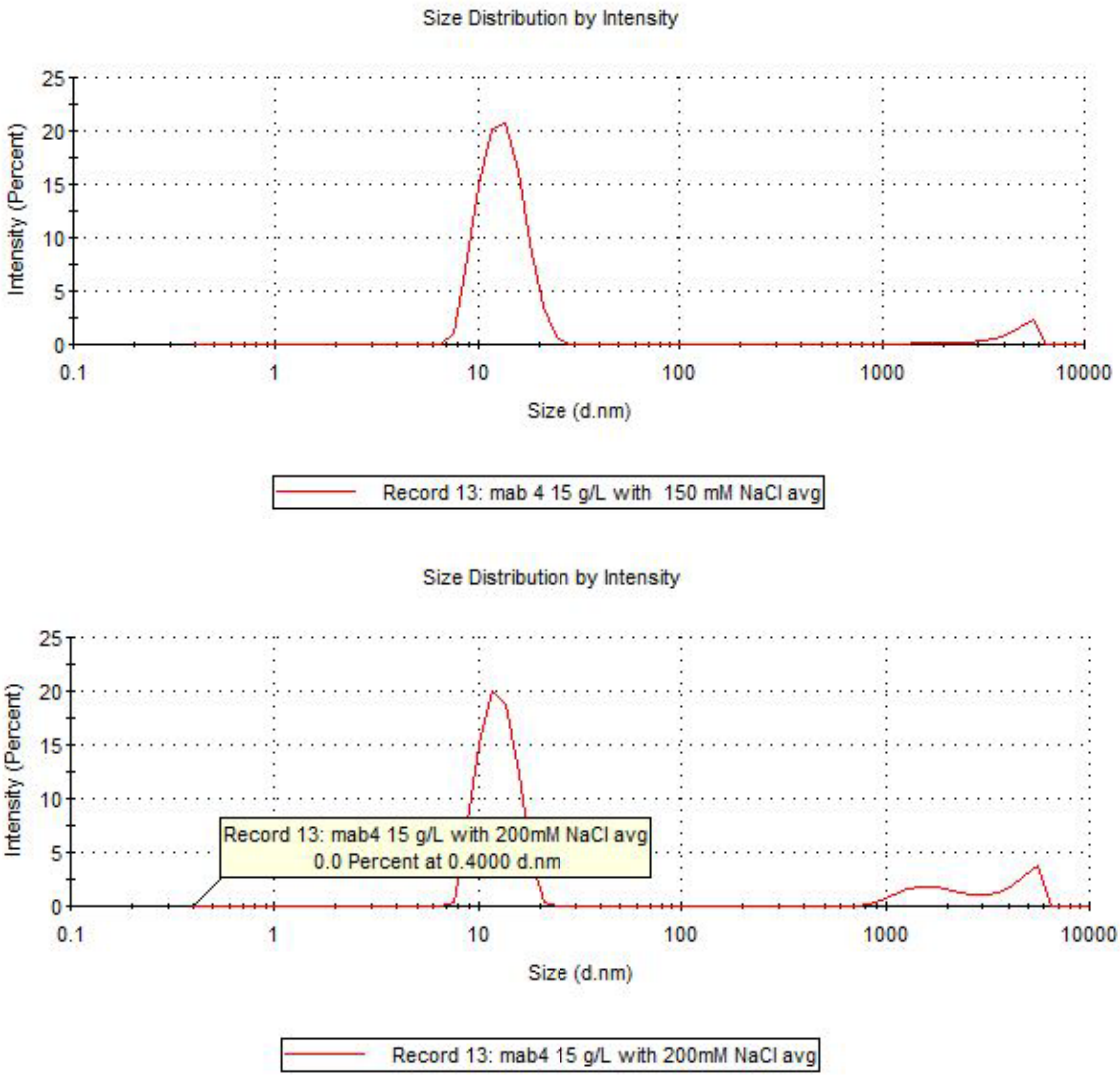

Figure 15. Size Distribution by Intensity Graphs for NaCl + mAb-4.

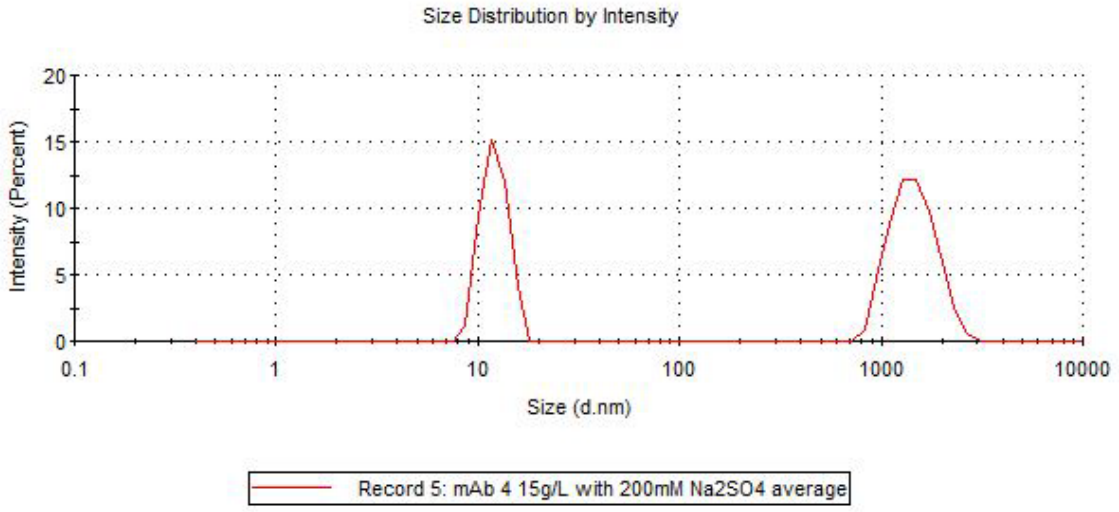
Size Distribution by Intensity
Intensity (Percent)
20
15
10
5
0
0.1
1
10
100
1000
10000
Size (d.nm)
Record 5: mAb 4 15g/L with 200mM Na2SO4 average

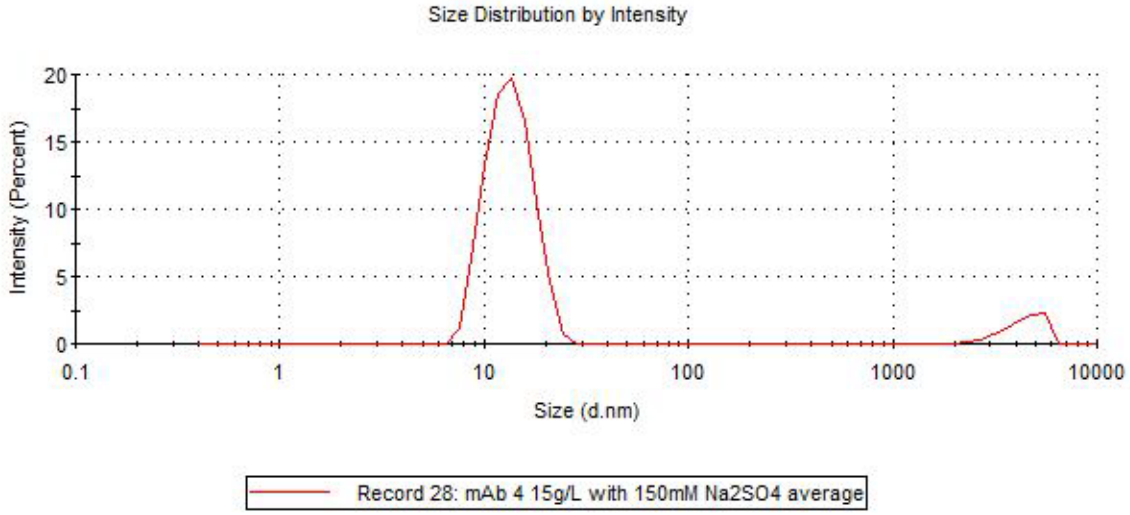
Size Distribution by Intensity
Intensity (Percent)
20
15
10
5
0
0.1
1
10
100
1000
10000
Size (d.nm)
Record 28: mAb 4 15g/L with 150mM Na2SO4 average

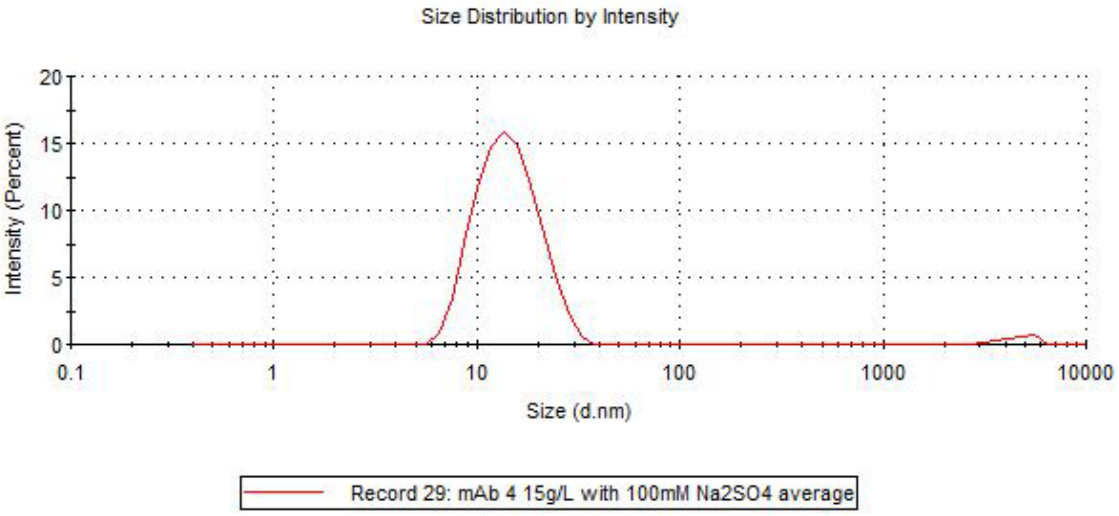
Size Distribution by Intensity
Intensity (Percent)
20
15
10
5
0
0.1
1
10
100
1000
10000
Size (d.nm)
Record 29: mAb 4 15g/L with 100mM Na2SO4 average

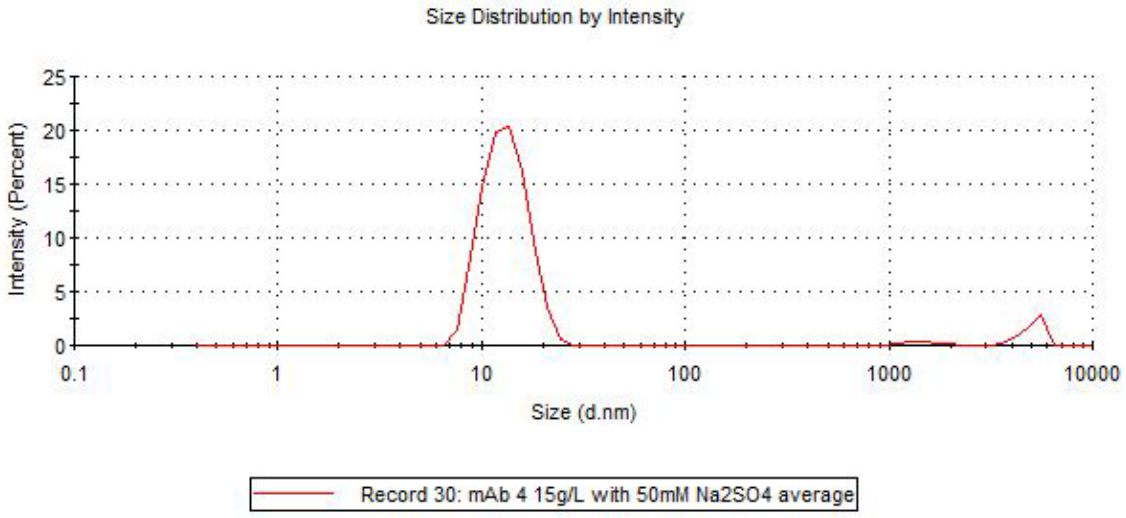
Size Distribution by Intensity
Intensity (Percent)
25
20
15
10
5
0
0.1
1
10
100
1000
10000
Size (d.nm)
Record 30: mAb 4 15g/L with 50mM Na2SO4 average

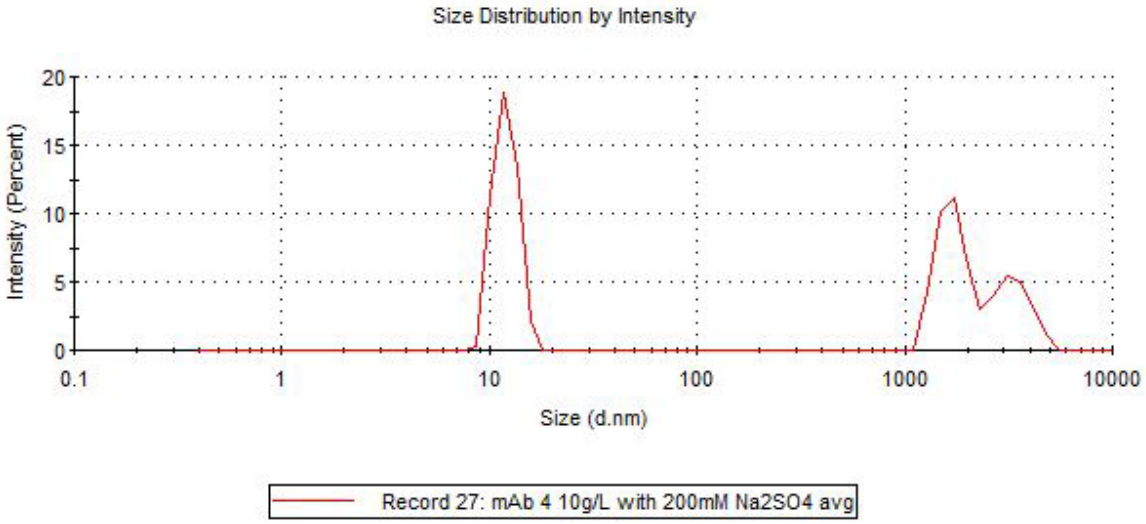
Size Distribution by Intensity
Intensity (Percent)
20
15
10
5
0
0.1
1
10
100
1000
10000
Size (d.nm)
Record 27: mAb 4 10g/L with 200mM Na2SO4 avg

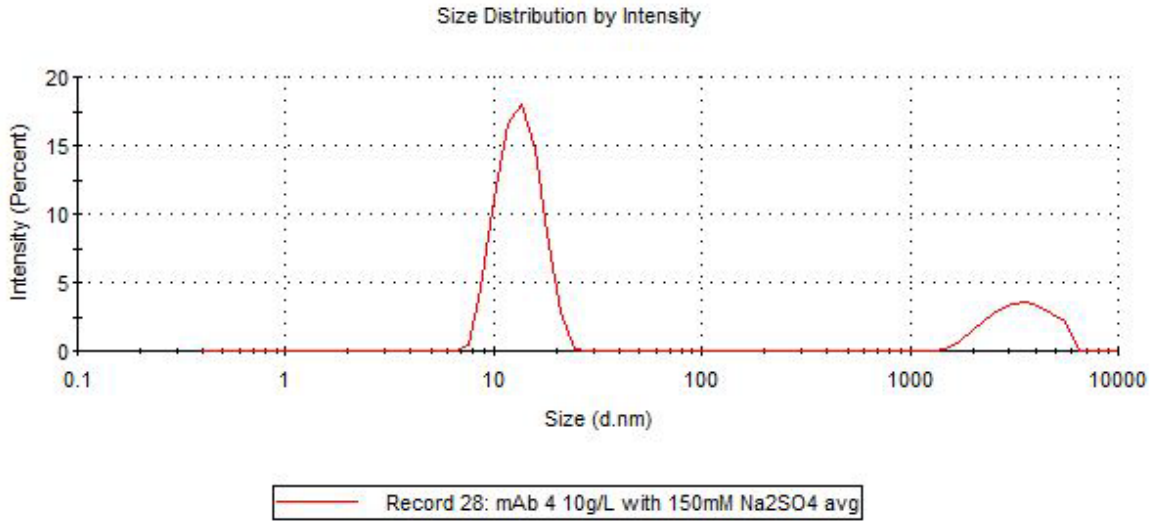
Size Distribution by Intensity
Intensity (Percent)
20
15
10
5
0
0.1
1
10
100
1000
10000
Size (d.nm)
Record 28: mAb 4 10g/L with 150mM Na2SO4 avg

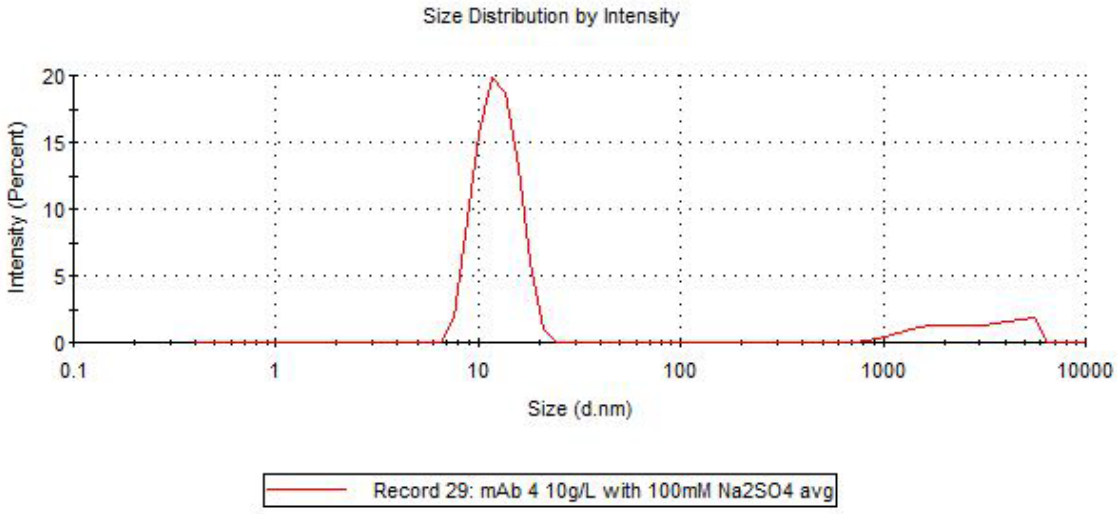
Size Distribution by Intensity
Intensity (Percent)
20
15
10
5
0
0.1
1
10
100
1000
10000
Size (d.nm)
Record 29: mAb 4 10g/L with 100mM Na2SO4 avg

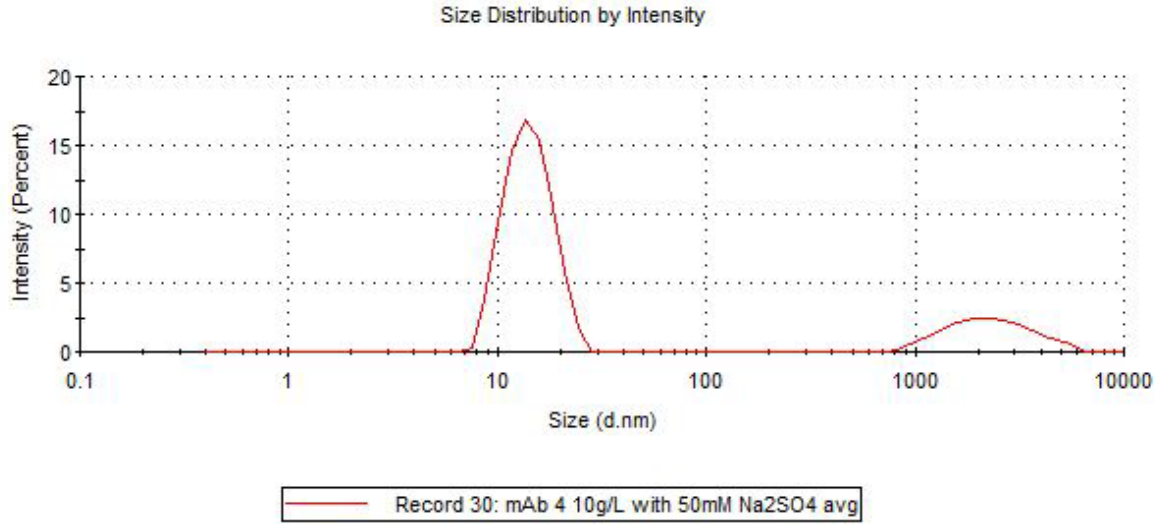
Size Distribution by Intensity
Intensity (Percent)
20
15
10
5
0
0.1
1
10
100
1000
10000
Size (d.nm)
Record 30: mAb 4 10g/L with 50mM Na2SO4 avg

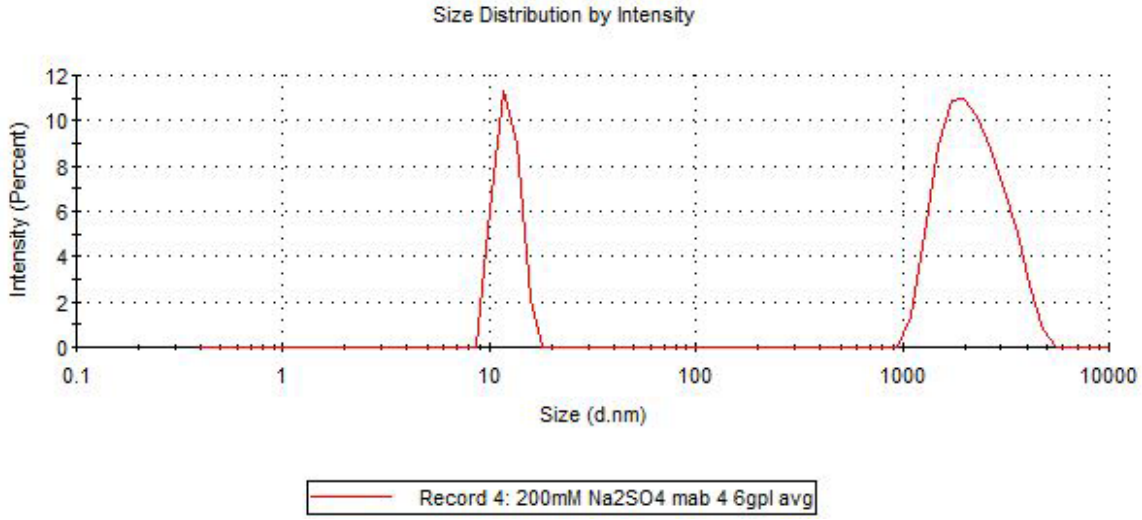
Size Distribution by Intensity
Intensity (Percent)
12
10
8
6
4
2
0
0.1
1
10
100
1000
10000
Size (d.nm)
Record 4: 200mM Na2SO4 mab 4 6gpl avg

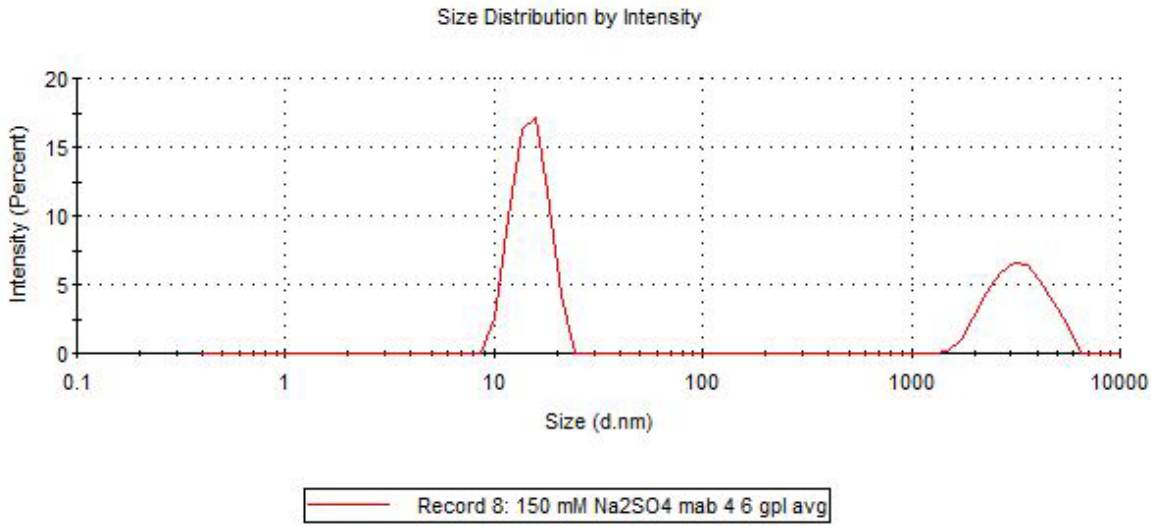
Size Distribution by Intensity
Intensity (Percent)
20
15
10
5
0
0.1
1
10
100
1000
10000
Size (d.nm)
Record 8: 150 mM Na2SO4 mab 4 6 gpl avg

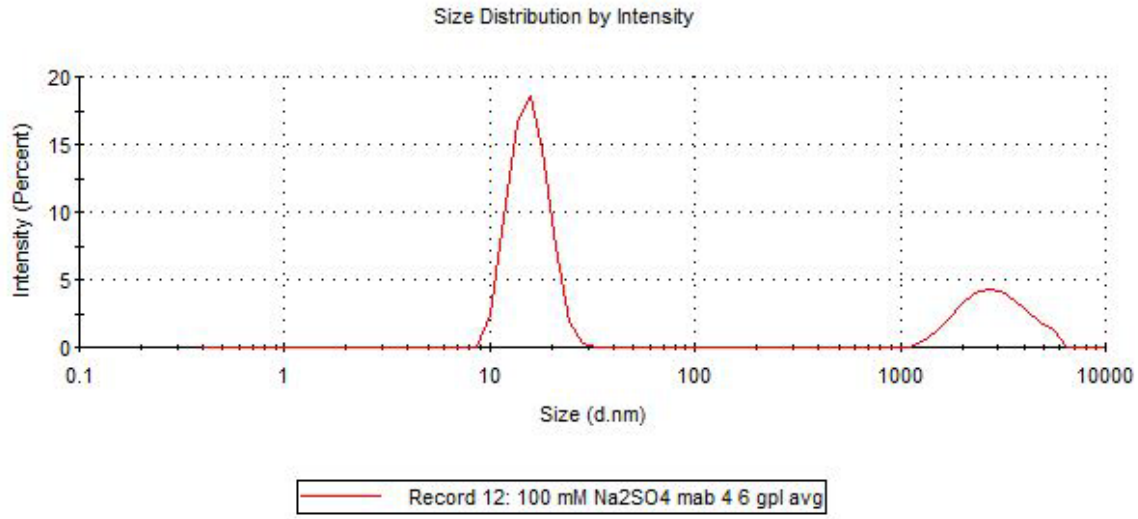
Size Distribution by Intensity
Intensity (Percent)
20
15
10
5
0
0.1
1
10
100
1000
10000
Size (d.nm)
Record 12: 100 mM Na2SO4 mab 4 6 gpl avg

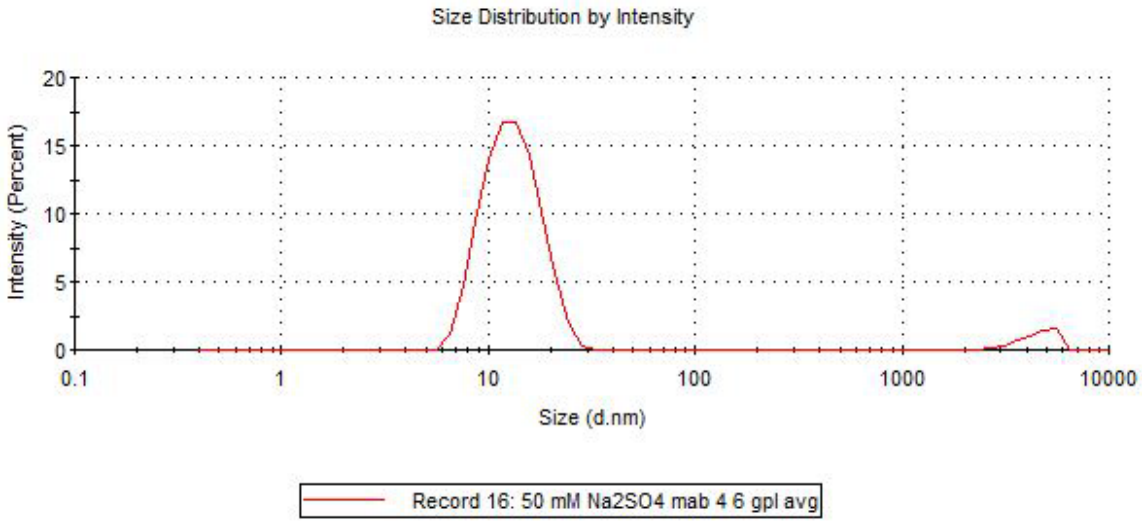
Size Distribution by Intensity
Intensity (Percent)
20
15
10
5
0
0.1
1
10
100
1000
10000
Size (d.nm)
Record 16: 50 mM Na2SO4 mab 4 6 gpl avg

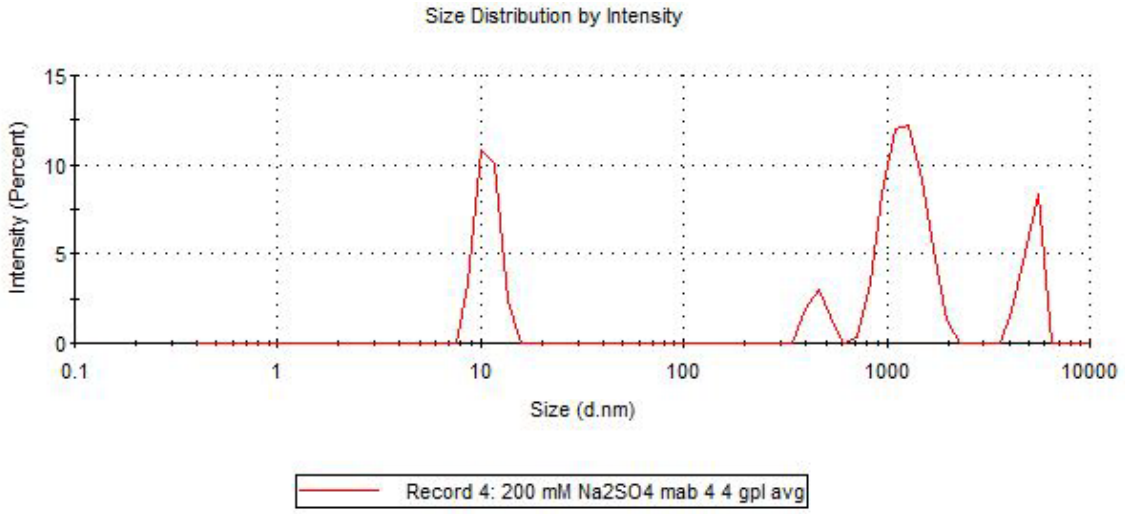
Size Distribution by Intensity
Intensity (Percent)
15
10
5
0
0.1
1
10
100
1000
10000
Size (d.nm)
Record 4: 200 mM Na2SO4 mab 4 4 gpl avg

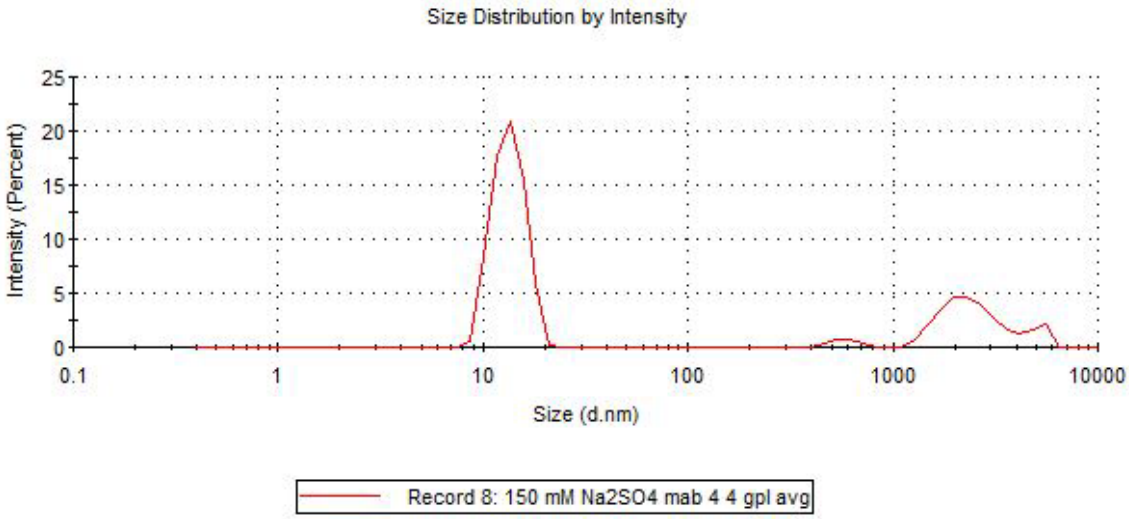
Size Distribution by Intensity
Intensity (Percent)
25
20
15
10
5
0
0.1
1
10
100
1000
10000
Size (d.nm)
Record 8: 150 mM Na2SO4 mab 4 4 gpl avg

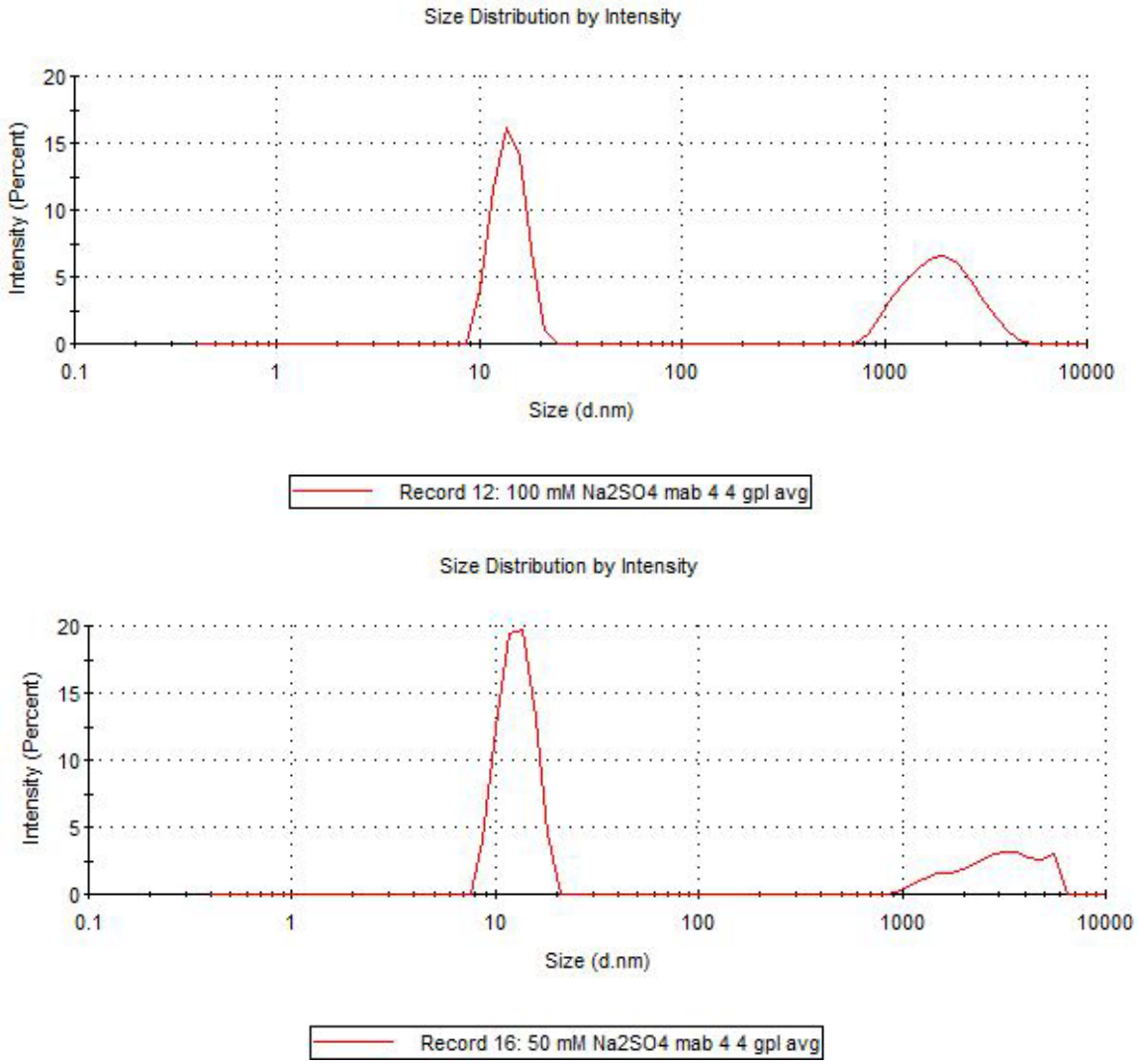

Figure 16. Size Distribution by Intensity Graphs for Na_2SO_4 + mAb-4.

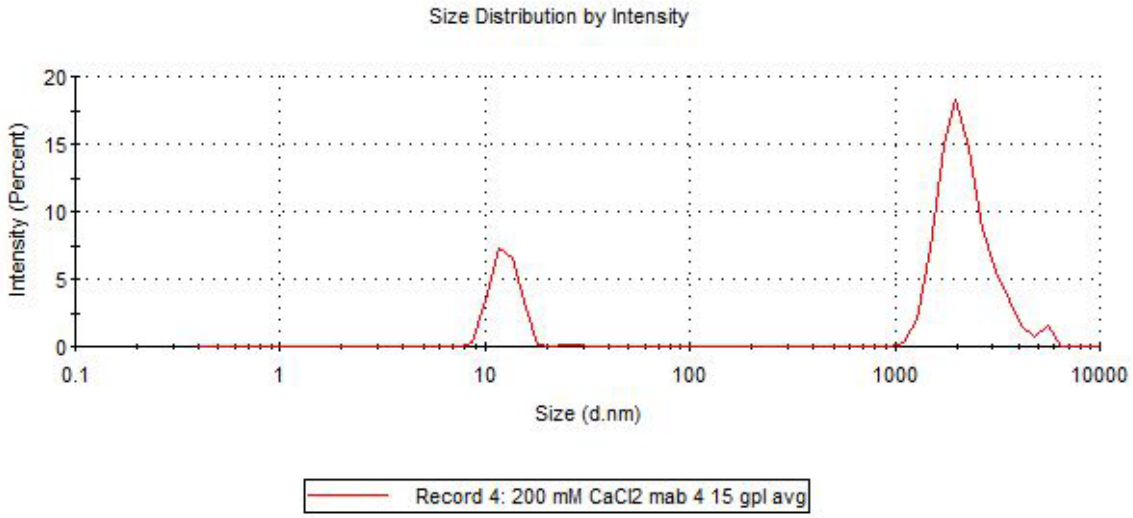
Size Distribution by Intensity
Intensity (Percent)
20
15
10
5
0
0.1
1
10
100
1000
10000
Size (d.nm)
Record 4: 200 mM CaCl2 mab 4 15 gpl avg

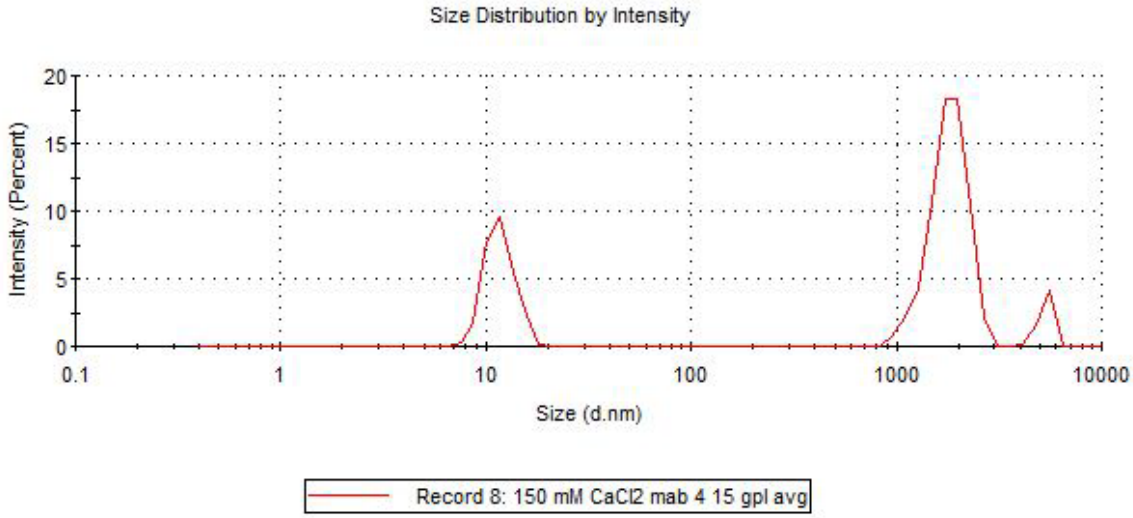
Size Distribution by Intensity
Intensity (Percent)
20
15
10
5
0
0.1
1
10
100
1000
10000
Size (d.nm)
Record 8: 150 mM CaCl2 mab 4 15 gpl avg

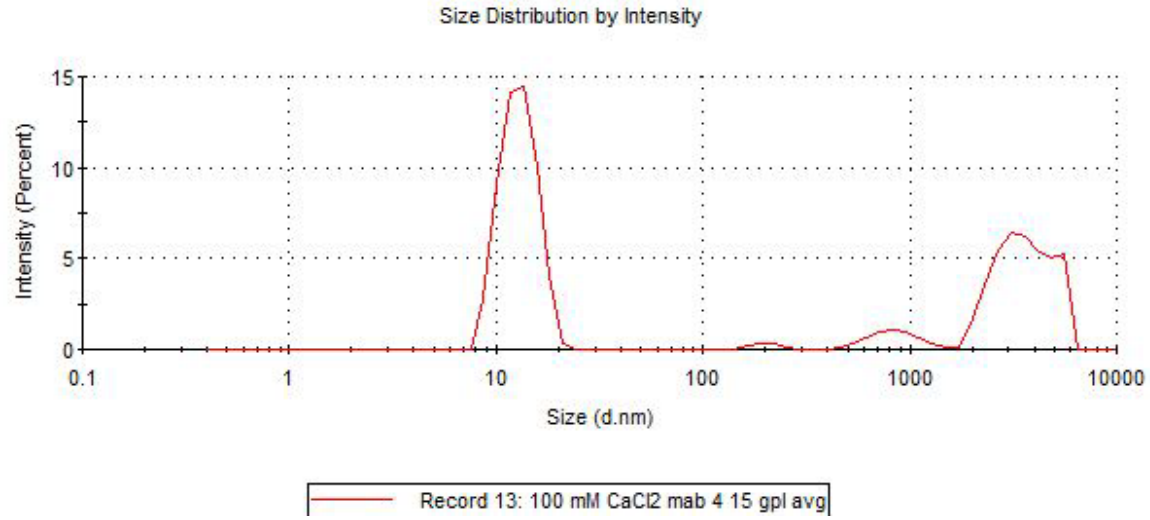
Size Distribution by Intensity
Intensity (Percent)
15
10
5
0
0.1
1
10
100
1000
10000
Size (d.nm)
Record 13: 100 mM CaCl2 mab 4 15 gpl avg

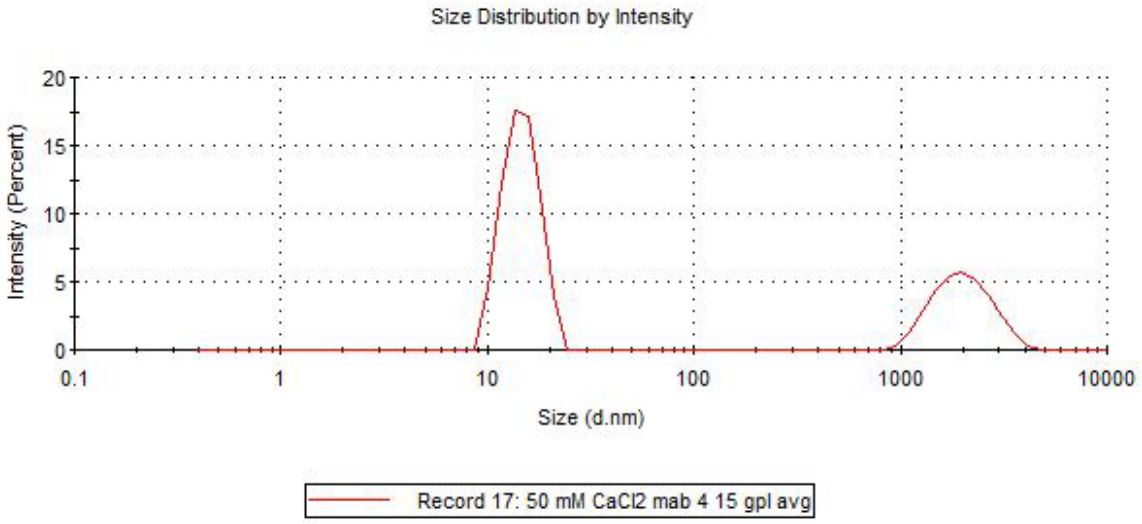
Size Distribution by Intensity
Intensity (Percent)
20
15
10
5
0
0.1
1
10
100
1000
10000
Size (d.nm)
Record 17: 50 mM CaCl2 mab 4 15 gpl avg

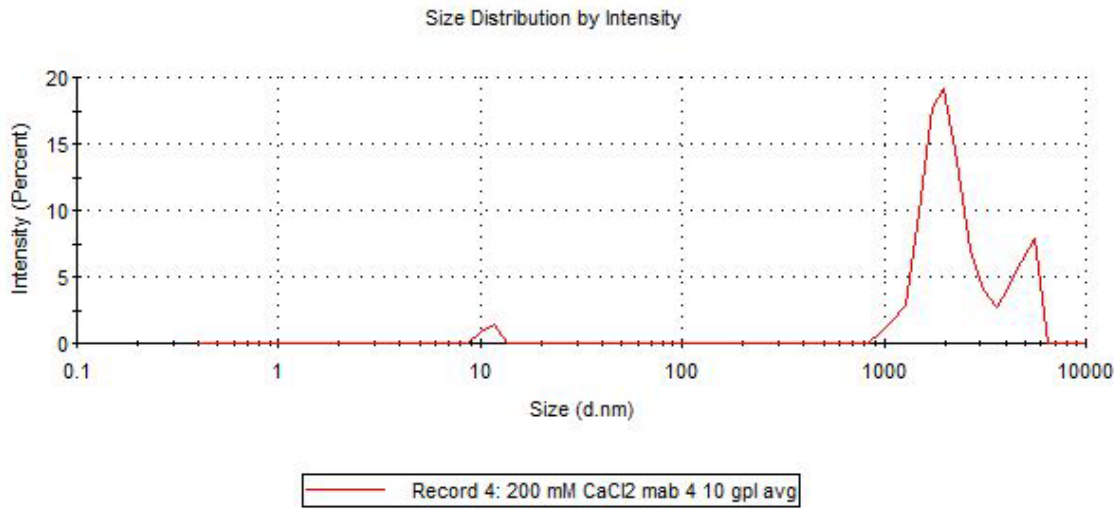
Size Distribution by Intensity
Intensity (Percent)
20
15
10
5
0
0.1
1
10
100
1000
10000
Size (d.nm)
Record 4: 200 mM CaCl2 mab 4 10 gpl avg

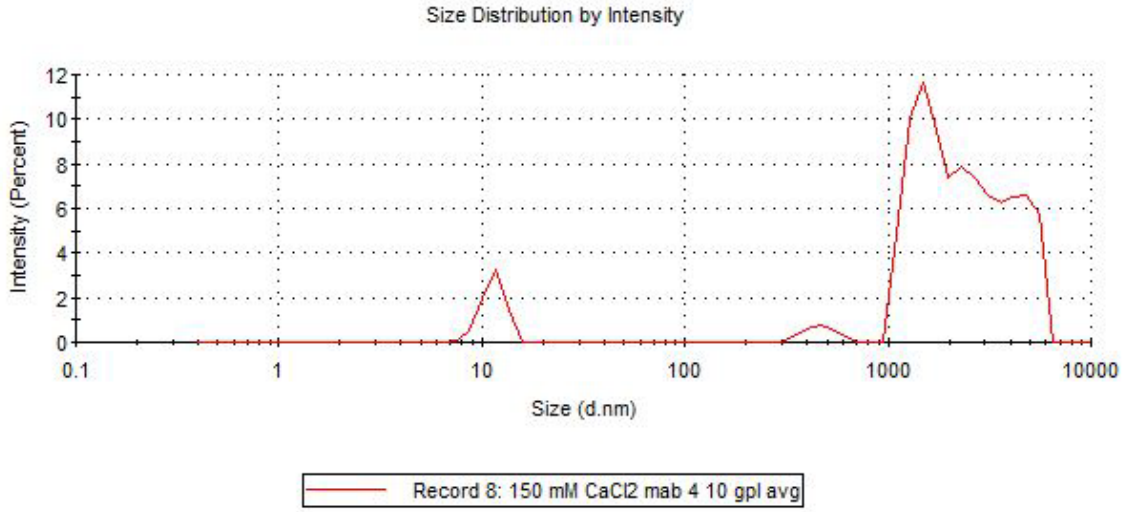
Size Distribution by Intensity
Intensity (Percent)
12
10
8
6
4
2
0
0.1
1
10
100
1000
10000
Size (d.nm)
Record 8: 150 mM CaCl2 mab 4 10 gpl avg

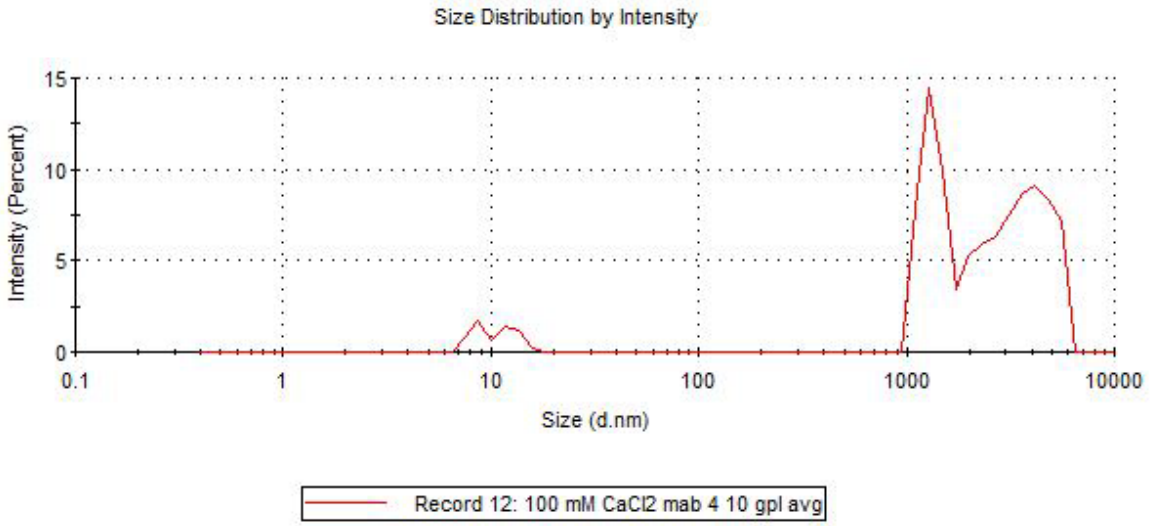
Size Distribution by Intensity
Intensity (Percent)
15
10
5
0
0.1
1
10
100
1000
10000
Size (d.nm)
Record 12: 100 mM CaCl2 mab 4 10 gpl avg

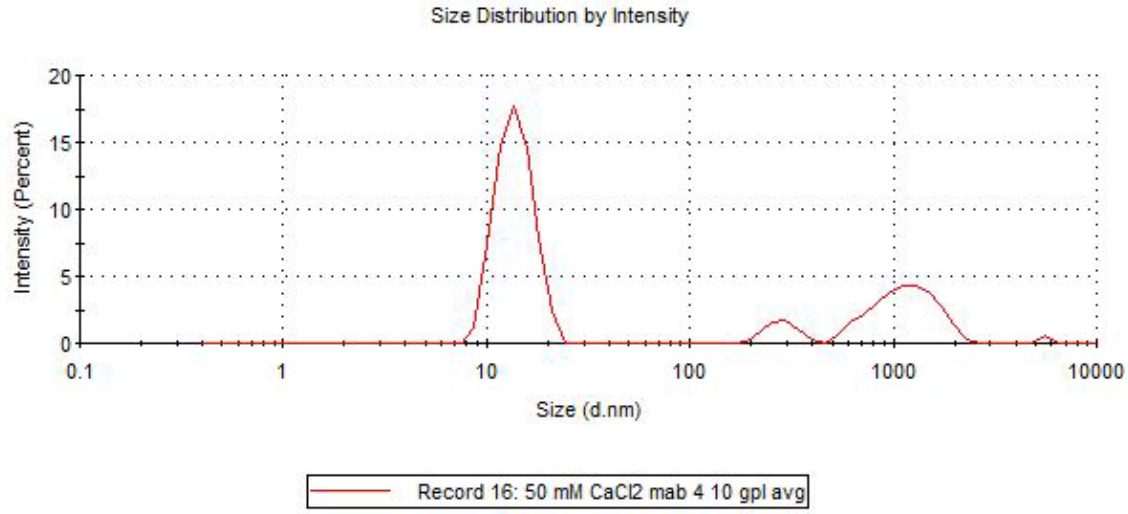
Size Distribution by Intensity
Intensity (Percent)
20
15
10
5
0
0.1
1
10
100
1000
10000
Size (d.nm)
Record 16: 50 mM CaCl2 mab 4 10 gpl avg

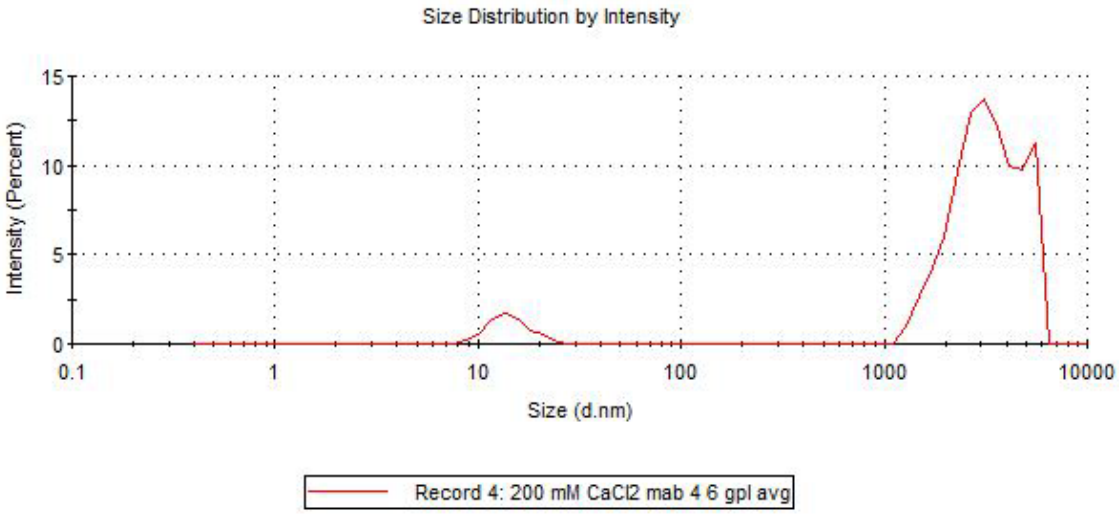
Size Distribution by Intensity
Intensity (Percent)
15
10
5
0
0.1
1
10
100
1000
10000
Size (d.nm)
Record 4: 200 mM CaCl2 mab 4 6 gpl avg

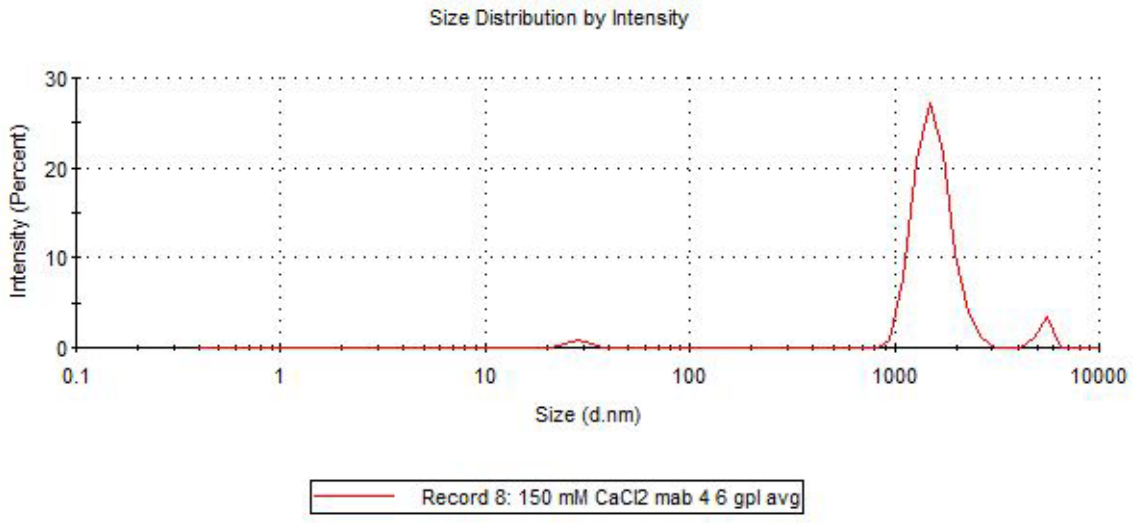
Size Distribution by Intensity
Intensity (Percent)
30
20
10
0
0.1
1
10
100
1000
10000
Size (d.nm)
Record 8: 150 mM CaCl2 mab 4 6 gpl avg

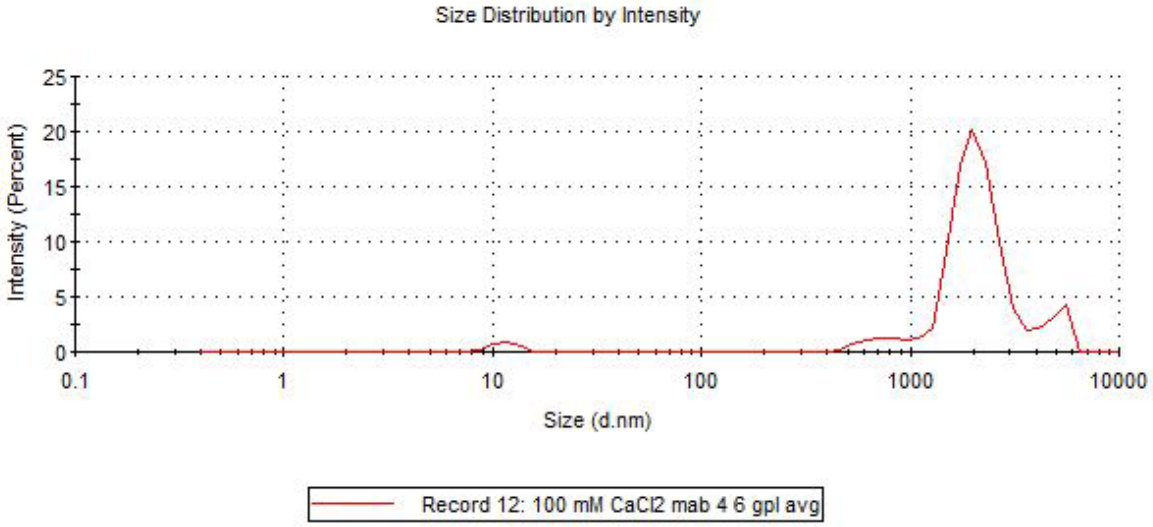
Size Distribution by Intensity
Intensity (Percent)
25
20
15
10
5
0
0.1
1
10
100
1000
10000
Size (d.nm)
Record 12: 100 mM CaCl2 mab 4 6 gpl avg

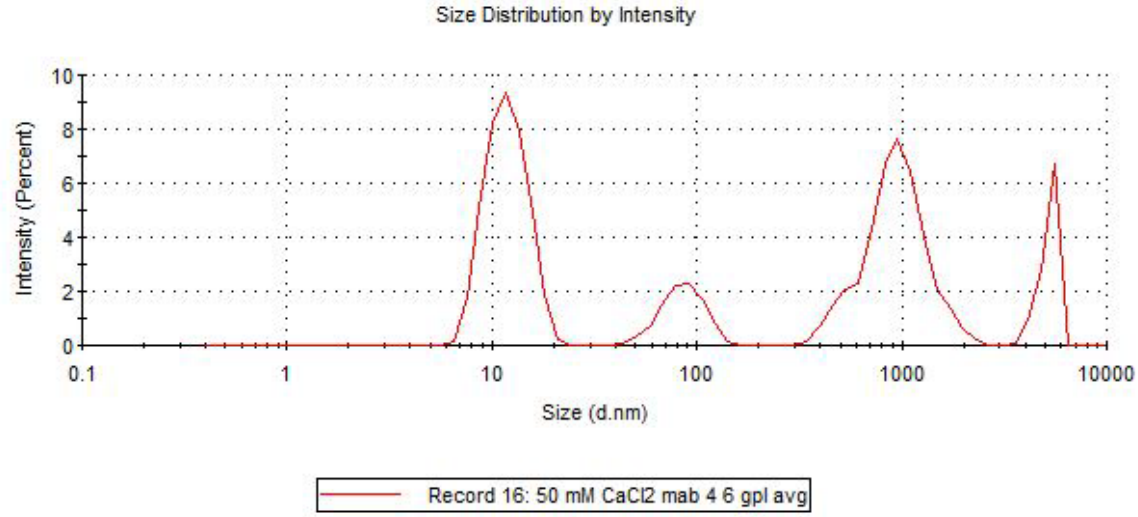
Size Distribution by Intensity
Intensity (Percent)
10
8
6
4
2
0
0.1
1
10
100
1000
10000
Size (d.nm)
Record 16: 50 mM CaCl2 mab 4 6 gpl avg

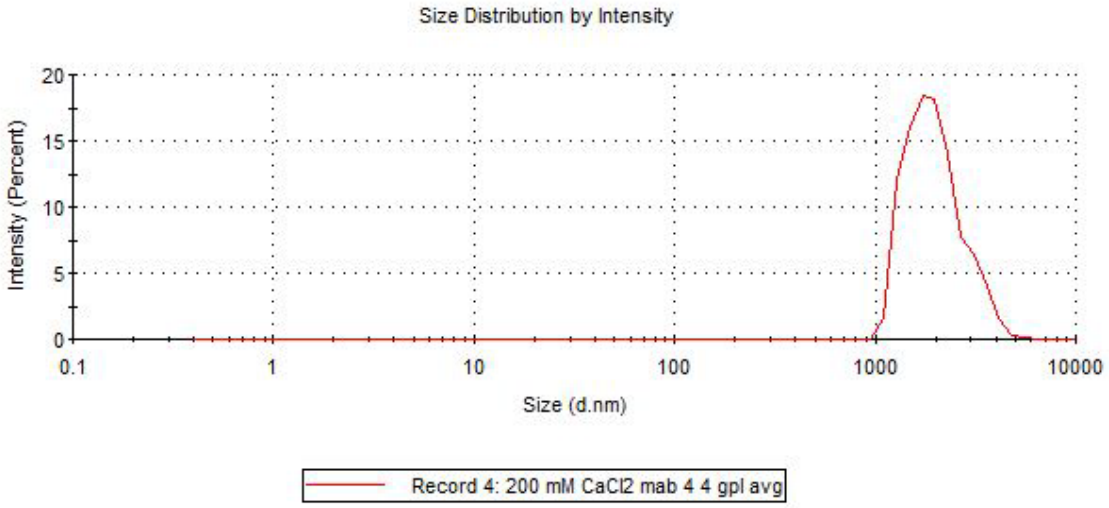
Size Distribution by Intensity
Intensity (Percent)
20
15
10
5
0
0.1
1
10
100
1000
10000
Size (d.nm)
Record 4: 200 mM CaCl2 mab 4 4 gpl avg

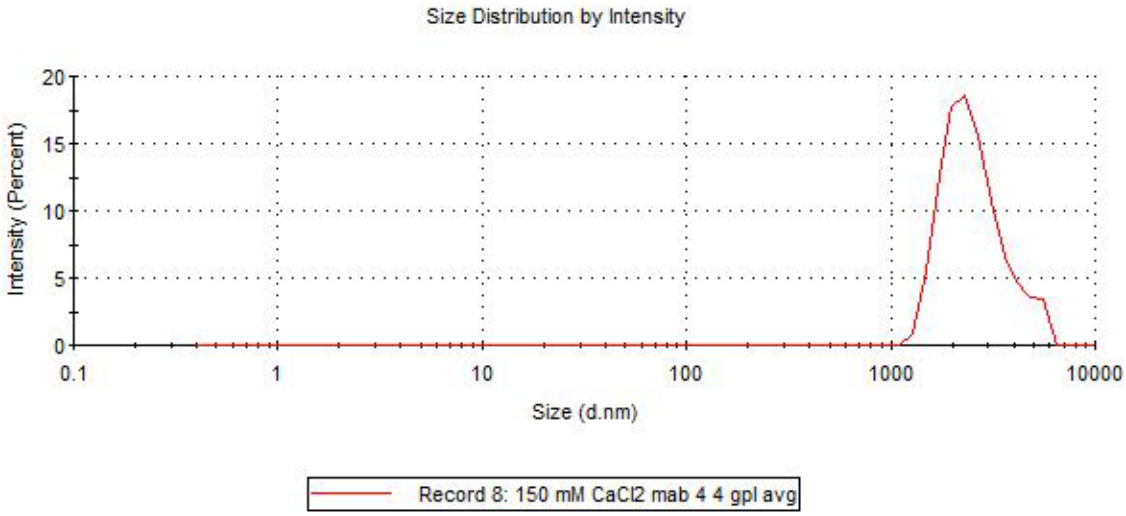
Size Distribution by Intensity
Intensity (Percent)
20
15
10
5
0
0.1
1
10
100
1000
10000
Size (d.nm)
Record 8: 150 mM CaCl2 mab 4 4 gpl avg

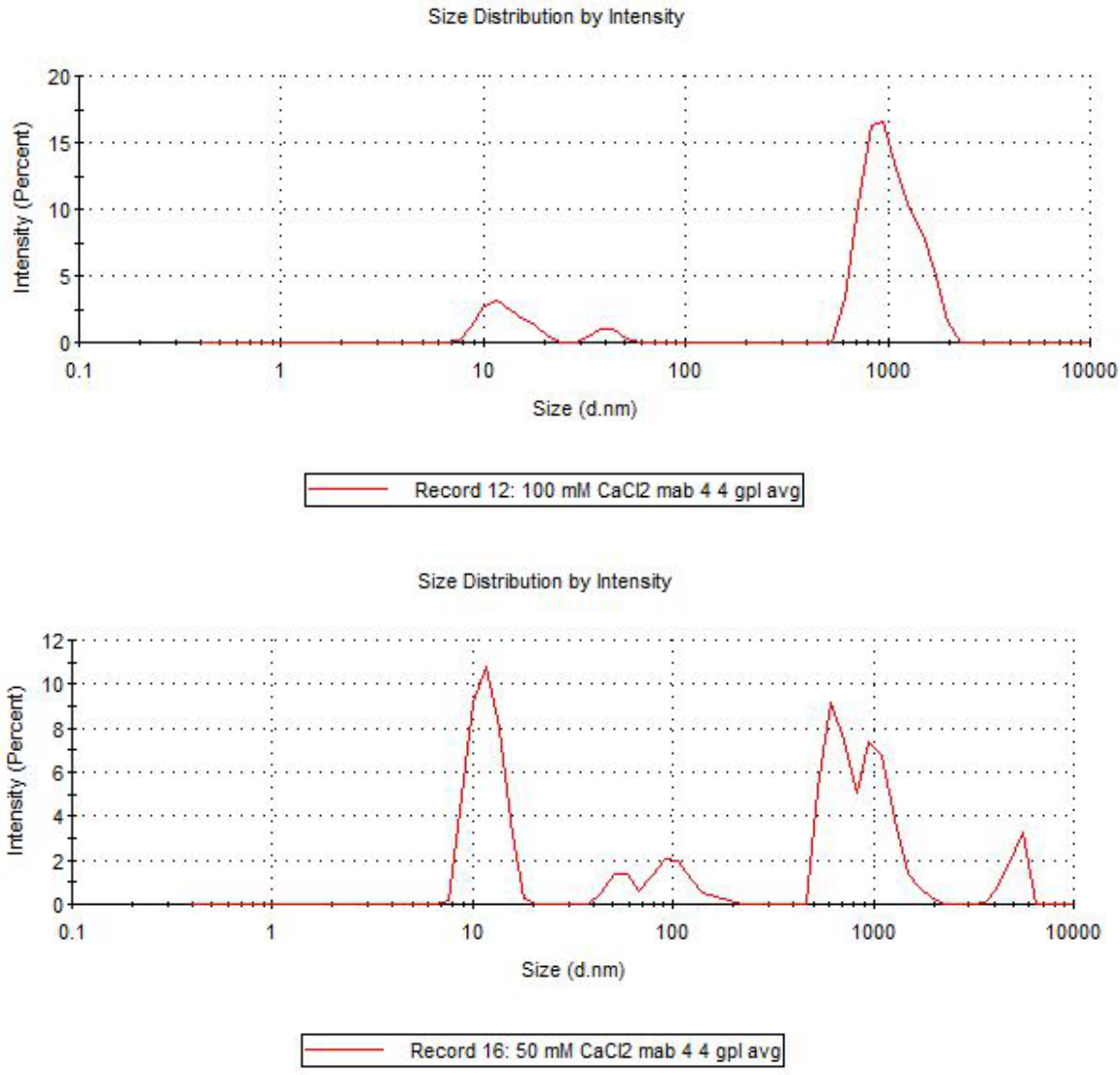

Figure 16. Size Distribution by Intensity Graphs for $CaCl_2$ + mAb-4.

BIBLIOGRAPHY

1. Reth, M. “Matching Cellular Dimensions with Molecular Sizes.” *Nature Immunology*, vol. 14, no. 8, 2013, pp. 765–767., https://doi.org/10.1038/ni.2621.
2. Janeway, CA, Travers, P., Walport, M., et al.“The Structure of a Typical Antibody Molecule”, in Immunobiology: The Immune System in Health and Disease, 5th Edition -.” *National Library of Medicine*, 2013, https://www.ncbi.nlm.nih.gov/books/NBK27144/.
3. “Antibody.” *Genome.gov*, 2010, https://www.genome.gov/genetics-glossary/Antibody.
4. “Monoclonal Antibodies.” *National Center for Biotechnology Information*, U.S. National Library of Medicine, 2012, https://pubmed.ncbi.nlm.nih.gov/31644151/.
5. Liu, J. K H. “The History of Monoclonal Antibody Development - Progress, Remaining Challenges and Future Innovations.” *Annals of Medicine and Surgery (2012)*, U.S. National Library of Medicine, 11 Sept. 2014, https://www.ncbi.nlm.nih.gov/pmc/articles/PMC4284445/.
6. Reichert, J. M., et al. “Monoclonal Antibody Successes in the Clinic.” *Nature Biotechnology*, vol. 23, 2005, pp. 1073-1078, https://www.nature.com/articles/nbt0905-1073.
7. “Monoclonal Antibodies Market Size & Share Report, 2030.” *Monoclonal Antibodies Market Size & Share Report, 2030*, Grand View Research, 2022, https://www.grandviewresearch.com/industry-analysis/monoclonal-antibodies-market.

8. Burnouf, T, and M Radosevich. “Nanofiltration of plasma-derived biopharmaceutical products.” *Haemophilia,* vol. 9,1 (2003): 24-37. doi:10.1046/j.1365-2516.2003.00701.x

9. “Monoclonal Antibody Downstream Processing.” *Removing Viruses from Your Downstream Mab Process*, Sigma Aldrich, 2023, https://www.sigmaaldrich.com/US/en/applications/pharmaceutical-and-biopharmaceutical-manufacturing/monoclonal-antibody-manufacturing/removing-viruses-downstream.

10. van Reis, R., Zydney, A. “Bioprocess membrane technology.” Journal of Membrane Science 297 (2007) 16–50

11. Pujar, N.S., Zydney, A.L., “Electrostatic effects on protein partitioning in size exclusion chromatography and membrane ultrafiltration”, J. Chromatogr. A 796 (1998) 229

12. Matusiak, J.. "Stability of Colloidal Systems - A Review of the Stability Measurements Method." *Researchgate.Net*, 1 Dec. 2017, www.researchgate.net/publication/321868250_Stability_of_colloidal_systems-a_review_of_the_stability_measurements_methods. 2023.

13. “Zetasizer | Expert Light Scattering Instruments | Malvern Panalytical.” *Www.malvernpanalytical.com*, www.malvernpanalytical.com/en/products/product-range/zetasizer-range.

14. “What Is the Z-Average?” *Malvernpanalytical.com*, 2023, www.malvernpanalytical.com/en/learn/knowledge-center/faqs/faq0015averagediameter.

15. *Dynamic Light Scattering: An Introduction in 30 Minutes*.

16. Kheddo, P., et al. "The Effects of Arginine Glutamate, a Promising Excipient for Protein Formulation, on Cell Viability: Comparisons with NaCl." *Toxicology in Vitro*, vol. 33, June 2016, pp. 88–98, https://doi.org/10.1016/j.tiv.2016.02.002.

17. Gregory, K. P., et al. "Understanding Specific Ion Effects and the Hofmeister Series." *Physical Chemistry Chemical Physics*, vol. 24, no. 21, 2022, pp. 12682–12718, https://doi.org/10.1039/d2cp00847e.

18. Boström, M., et al., "Why forces between proteins follow different Hofmeister series for pH above and below pI." *Biophys Chem* **117**, 217–224 (2005).

19. Velegol, D. *Colloidal Systems*. United States, Wild Scholars Media, 2016.

ACADEMIC VITA

Thomas R. Butts Jr.

TPB5474@psu.edu

EDUCATION

The Pennsylvania State University, Schreyer Honors College — **University Park, PA**
College of Engineering — ***August 2020 – May 2023***
Bachelor of Science in Chemical Engineering

INTERNSHIP EXPERIENCE

Material Science and Technology Intern at Merck — **Millsboro, DE**
May 2022 – August 2022

- Collaborated on a project to decrease costs and risks associated with manufacturing of BRSV vaccine.
- Authored, edited, and reviewed Standard Operating Procedure (SOP) documentation.
- Generated data by conducting various pilot-scale laboratory experiments and performed statistical analyses to determine the feasibility of changes to manufacturing process.
- Participated in equipment validation for pumps, filtration devices, tanks, and heat exchangers.
- Implemented changes to manufacturing procedures, resulting in thousands of dollars saved annually.

THESIS & PROJECT EXPERIENCE

Liquid Natural Gas Project — **University Park, PA**
Principal Researcher and Author — *August 2022-December 2022*

- Investigated various separation processes to purify a methane-CO_2 stream.
- Performed adsorption, cryogenic distillation, and filtration simulations in ASPEN HYSYS to determine optimal method of separation. Selected a process to yield optimal profitability.
- Created a comprehensive P&ID/simulation for obtaining LNG via cryogenic distillation.
- Authored a report detailing the HYSYS simulation and recommendations for process & safety design.

Penn State Bioprocessing Lab for Therapeutic Proteins (Zydney Lab) — **University Park, PA**
Research Assistant to Dr. Andrew Zydney — *August 2021 – Present*
Thesis Topic: Optimization of Ultrafiltration of Monoclonal Antibody Products

- Collaborated on research focusing on fouling behaviors of monoclonal antibody products and virus removal filtration for the manufacturing of safe bioproducts.
- Conducted independent thesis research by authoring procedures to extract desired data.
- Authored various technical documents to report findings (reports, theses, presentations, etc.).

Teaching Assistant in Department of Chemical Engineering — **University Park, PA**
Teaching Assistant in CHE 230, Computational Tools — *August 2021 – Present*

- Developed curriculum and instructed a course concerning data analysis and computational tools used for engineering applications. Requires expertise in Excel, ASPEN HYSYS, and Mathematica.

EXTRACURRICULAR ACTIVITIES/COURSEWORK

American Institute of Chemical Engineers (AICHE) — **University Park, PA**
Fundraising Chair for THON/Member — *September 2022 – Present*

- Lead and organized fundraising events to raise money for THON. Corresponded with local businesses to promote AICHE's THON organization.

RELEVANT SKILLS AND COURSEWORK P&ID design, safety design, reactor engineering, thermodynamics, heat transfer, mass transfer, multi- variable calculus, statistics, fluid mechanics.

Certifications: ELA984: Inherently Safer Design, ELA975: Process Safety Ethics, ELA969: Understanding Hazards & Risks, SAChE964: Explosion Hazards, ELA962: Chemical Reactivity Hazards, SAChE963: Fire Hazards